



UiT The Arctic University of Norway

Faculty of Health Sciences

Department of Pharmacy

Drug Transport and Delivery Research Group

**Dual delivery of chlorogenic acid and mimic of antimicrobial peptide –
towards wound treatment**

Mari Salamonsen

Thesis for the degree Master of Pharmacy 2022

MASTER THESIS FOR THE DEGREE MASTER OF PHARMACY
DUAL DELIVERY OF CHLOROGENIC ACID AND MIMIC OF ANTIMICROBIAL
PEPTIDE – TOWARDS WOUND TREATMENT

BY

MARI SALAMONSEN

MAY 2022

SUPERVISORS

Ph.D. candidate Lisa Myrseth Hemmingsen

and

Professor Nataša Skalko-Basnet

Drug Transport and Delivery Research Group

Department of Pharmacy

Faculty of Health Sciences

UiT The Arctic University of Norway

Acknowledgement

Work for the following thesis was carried out at the Drug Transport and Delivery Research Group, Department of Pharmacy, UiT The Arctic University of Norway in the period from August 2021 to May 2022.

First and foremost, I would like to express my deepest gratitude to my supervisor, Ph.D. candidate Lisa Myrseth Hemmingsen. Thank you for the support and guidance, and for always being there whenever I had questions or problems in the lab. Your help and advice have been invaluable throughout this year.

I would also like to extend my appreciation to my supervisor Professor Nataša Skalko-Basnet for overseeing my work, motivating me and encouraging me to seek out new knowledge.

I would like to thank the whole Drug Transport and Delivery Research Group for helping me out and creating a great environment for learning. Hereunder, I would like to give a special thanks to our engineer Cristiane de Albuquerque Cavalcanti Jacobsen for your technical help and encouragement throughout the year.

In addition, a thank you to the Host Microbe Interactions Research Groups and Women's Health and Perinatology Research Group, for letting me work in your laboratories during this project.

I would like to thank Lipoid GmbH for providing lipids and Chitinor AS for providing chitosan for this project.

Finally, I wish to express my deepest gratitude towards my parents and the rest of my family for their encouragement throughout my studies. Thank you for always being there for me.

Mari Salamonsen

May 2022

Table of Contents

1	General introduction.....	1
2	Introduction	3
2.1	Skin.....	3
2.1.1	Wound healing	5
2.2	Chronic wounds.....	6
2.2.1	Inflammation in chronic wounds.....	6
2.2.2	Infections in chronic wounds	7
2.2.3	Treatment of chronic wounds.....	7
2.3	Biofilms.....	8
3	Active compounds.....	10
3.1	Antimicrobial peptides	10
3.2	Chlorogenic acid	12
4	Drug delivery system	13
4.1	Dermal drug delivery	13
4.2	Liposomes	14
4.2.1	Effect of liposomal size on nanoscale	15
4.2.2	Effect of liposomal charge	16
4.3	Hydrogel.....	17
4.3.1	Chitosan in hydrogel	17
4.3.2	Liposomes-in-hydrogel	19
4.3.3	Texture properties of hydrogel.....	20
5	Aim of the study.....	23
6	Materials.....	24
6.1	Materials.....	24
6.2	Equipment	25
6.3	Instruments.....	26

6.4	Software	27
6.5	Biologicals.....	27
7	Methods.....	28
7.1	Preparation of empty liposomes.....	28
7.2	Preparation of drug-loaded liposomes.....	28
7.3	Size reduction of liposomes: Membrane extrusion	28
7.4	Characterization of liposomes.....	29
7.4.1	Analysis of vesicle size and polydispersity index.....	29
7.4.2	Zeta potential.....	29
7.4.3	pH.....	29
7.4.4	Entrapment efficiency	29
7.5	Hydrogel preparation.....	31
7.5.1	Plain chitosan hydrogel	31
7.5.2	Liposomes in chitosan hydrogel.....	31
7.5.3	Chitosan hydrogel with free drug.....	31
7.6	Hydrogel characterization	33
7.6.1	Viscosity.....	33
7.6.2	Texture analyser	33
7.7	pH.....	33
7.8	Stability testing of liposomes and hydrogels.....	33
7.8.1	Stability of liposomes.....	34
7.8.2	Stability of hydrogel.....	34
7.9	<i>In vitro</i> release study: Franz cell diffusion.....	34
7.10	Anti-oxidative activity.....	35
7.10.1	DPPH Radical Scavenging.....	35
7.10.2	ABTS•+ Radical Scavenging Activity	35
7.11	Evaluation of cell compatibility	35

7.12	Antimicrobial evaluation.....	36
7.13	Statistical analyzes	38
8	Results and discussion.....	39
8.1	Liposome vesicle characteristics and stability	39
8.1.1	Size	39
8.1.2	Zeta potential.....	41
8.1.3	pH.....	42
8.1.4	Liposomal entrapment of active compounds	43
8.2	Hydrogel characteristics	44
8.2.1	pH of hydrogel	44
8.2.2	Viscosity.....	46
8.2.3	Texture properties	48
8.3	<i>In vitro</i> release study: Franz cell diffusion.....	50
8.4	Anti-oxidative activity.....	52
8.5	Cell compatibility	54
8.6	Antimicrobial testing.....	56
9	Conclusion.....	59
10	Perspectives.....	60
11	References	61
12	Appendix	65
	Appendix I: Stability testing of texture properties	65
	Appendix II: Antimicrobial testing	67

List of Tables

Table 1: Programmed flow for mobile phase distribution in HPLC analysis	30
Table 2: Overview of studied hydrogel formulations and their components	32
Table 3: Formulations included in in vitro drug release testing by Franz cell diffusion.	34
Table 4: Overview of formulations in antimicrobial testing and their respective drug concentrations.....	37
Table 5: Size and size distribution for liposomal drug formulations over a period of 12 weeks. Each formulation was tested in 3 separate batches, with 3 measurements per batch. All values are expressed as mean \pm SD (n=3). Diameter measurement is intensity weighted. Week 0 = two days after production, one day after extrusion.	40
Table 6: Zeta potential of liposomal suspensions. Results are presented as mean with associated SD, n=3.	42

List of Figures

Figure 1: Cross-section of the skin structure, displaying the three skin layers, epidermis, dermis and hypodermis. Several structures, such as blood vessels, sensory nerve endings, hair follicles and sweat- and sebaceous glands, are embedded in the different layers of skin.....	3
Figure 2: Illustration of the stratum corneum with the brick and mortar model. The stratum corneum is the outermost layer of the epidermis. The bricks represent the corneocytes embedded the mortar, an intracellular lipid matrix	4
Figure 3: The four continuous and overlapping phases of wound healing; hemostasis, inflammation, proliferation and remodeling. The figure illustrates when the different phases are contributing to healing over the timespan of the healing process	5
Figure 4: Stages in biofilm formation. (1) Free planktonic bacteria adhere to surface, forming the biofilm. (2) Growth and maturation of the biofilm. The polymeric substances grant improved adhesion and protection, making eradication challenging. (3) Free bacteria are released from the biofilm to continue colonization.....	9
Figure 5: Proposed mechanisms of membrane interaction between AMPs and bacterial cell membrane. The prior conformational change is essential for the suggested mechanisms.....	11
Figure 6: Chemical structure of chlorogenic acid including pKa values for the carboxyl group and first phenolic group.....	12
Figure 7: General structure of unilamellar liposome showing the arrangement of phospholipid bilayer. Location of incorporated molecules, such as active compounds, is dependent on their hydrophilicity or lipophilicity, and consequently the ability to solubilize in the liposomal region of question.....	14
Figure 8: Chemical structure of chitin and chitosan. Chitosan is shown as partially deacetylated, and consists of both D-glucosamine and N-acetyl-glucosamine. Degree of deacetylation and molecular weight of the chitosan polymer can vary depending on the conditions used for deacetylation.....	18
Figure 9: Liposome-in-hydrogel network as a primary and secondary vehicle for effective drug delivery.	20
Figure 10: Texture properties on a force-time plot from the texture analysis of arbitrary chitosan hydrogel. The x-axis represents time, the y-axis force. The peak positive force, hardness, represents maximum compression force. Positive area under the curve is cohesiveness and negative area under the curve is adhesiveness.....	21

Figure 11: pH of all tested liposomal suspensions followed up for 12 weeks after production. Results are presented as mean \pm SD, n=3.	42
Figure 12: Entrapment of active compounds in liposomes, both as single- and dual-loaded formulations. Entrapment efficiency is given as a percentage of the amount of drug entrapped in liposomes compared to the total amount drug in the respective samples. Results are expressed as mean \pm SD, n=3.....	44
Figure 13: pH of liposome-in-chitosan-hydrogel formulations over the stability testing period of 12 weeks. Results are presented as mean \pm SD, n=3.	45
Figure 14: Shear rate plotted against shear stress for three different hydrogel formulations at 25 °C and 32 °C.	46
Figure 15: Viscosity plotted against shear stress for three different hydrogel formulations at 25 °C and 32 °C.	47
Figure 16: Comparison of texture properties at 2 weeks after production. Results are presented as mean \pm SD, n=3. * p<0.05 compared to empty chitosan hydrogel.	48
Figure 17: Comparison of texture properties at 12 weeks after production. Results are presented as mean \pm SD, n=3. * p<0.05 compared to empty chitosan hydrogel.	49
Figure 18: Drug release from liposomal suspensions and liposome-in-hydrogel formulations over 24 hours at 32 °C. The release is presented as a percentage of the total amount of entrapped drug, calculated from the amount established through entrapped testing. Results are expressed as mean \pm SD, n=3.....	50
Figure 19: Release of 8b from liposome-in-hydrogel formulation loaded with both CGA and 8b over a 24-hour period. The release is presented as a percentage of the total amount of entrapped drug, calculated from the amount established amount through entrapped testing. Results are expressed as mean \pm SD, n=3.	51
Figure 20: Anti-oxidative activity of CGA compared to vitamin C and E in ABTS radical scavenging. Results are expressed as mean \pm SD, n=2. All antioxidants were tested at concentration 50 μ M, 25 μ M, 10 μ M and 5 μ M. * p<0.05 compared to CGA in corresponding concentration.	52
Figure 21: Anti-oxidative activity of CGA compared to vitamin C and E in DPPH radical scavenging. Results are expressed as mean \pm SD, n=2. All antioxidants were tested at concentration 25 μ M, 10 μ M and 5 μ M. * p<0.05 compared to CGA in corresponding concentration.	53
Figure 22: Results of cell toxicity testing of liposomal suspensions on macrophages. Diluted formulations were added on the plates, resulting in an end lipid concentration of 50 μ g/mL, 10	

$\mu\text{g/mL}$ and $1 \mu\text{g/mL}$ in the wells. Results are expressed as the percentage of cell survival in treated cells compared to untreated cells. Results are presented as mean \pm SD, n=3. 54

Figure 23: Results of cell toxicity testing of liposome-in-hydrogel formulations on macrophages. Diluted formulations were added on the plates, resulting in an end lipid concentration of $50 \mu\text{g/mL}$, $10 \mu\text{g/mL}$ and $1 \mu\text{g/mL}$ in the wells. Results are expressed as the percentage of cell survival in treated cells compared to untreated cells Results are presented as mean \pm SD, n=3. 55

Figure 24: Antibacterial activity of liposome-in-chitosan-hydrogel formulations compared to a chitosan hydrogel with free active compounds. The antibacterial activity is expressed as the percentage of inhibition area for respective formulations compared to positive controls (100%). Results are expressed as mean \pm SD, n=3. * $p < 0.05$ compared to empty chitosan hydrogel (HG 1:4). 57

Abstract

Chronic wounds are a major burden, causing both morbidity and mortality in patients, as well as a massive economical strain on health care systems worldwide. These wounds have a high degree of complexity and are often difficult to treat due to the many factors limiting healing, such as inflammation, biofilm formation and bacterial infections. With these typically persistent infections and a rising threat of antibiotic resistance, there is an urgent need for new and effective dermal antimicrobial treatments. One group of novel antibiotics gaining focus in recent years is antimicrobial peptides (AMPs). Utilization of these compounds could be promising for the treatment of skin infections, but for chronic wounds, effective treatment through single target therapeutics is unlikely. The aim of this project was therefore to develop a novel dermal drug delivery system able to both eradicate bacterial skin infections and improve healing in chronic wounds. This was done by combining chlorogenic acid (CGA) and a synthetic mimic of an antimicrobial peptide in a liposome-in-hydrogel formulation with a bioactive polymer.

The CGA and our AMP called 8b were both single- and dual-loaded into liposome vesicles. Testing of relevant properties was done over a 12-week period to assess both stability and the drug delivery systems ability to deliver an effective and safe treatment to the skin. Straight after production, the dual-loaded liposomes had a mean vesicle size at 208 ± 2.5 nm with a polydispersity index (PI) of 0.083 ± 0.017 , zeta potential of 40.0 ± 1.3 mV and a pH of 3.00 ± 0.02 . Entrapment of active compound was more effective in dual-loaded liposomes than single-loaded, with an entrapment efficiency at 43.5% for CGA and 80.2% for the AMP 8b. All properties of the liposomal suspension showed adequate stability over the 12 weeks.

Liposomal suspensions were incorporated in a chitosan hydrogel and characterized over a 12-week period. The pH was stable at approximately 4.8 under the storage period. Rheological testing showed a pseudoplastic flow, fitting for dermal application. Measurement of texture properties for liposome-in-hydrogel showed that formulations incorporating CGA had significant changes in both hardness and cohesiveness between 4 and 12 weeks. Characterization of release from the liposome-in-hydrogel formulation showed a sustained release of 8b, but an inability of detectable CGA release. The antioxidant activity of CGA was characterized as comparable to well-known antioxidants vitamin C and E. Testing of cellular compatibility showed an unexpected toxic effect on murine macrophages for more highly concentrated hydrogels and formulations incorporating CGA. Both plain chitosan hydrogel and

the liposome-in-hydrogel formulations showed effective inhibition of bacterial growth in gram-positive and gram-negative bacteria, but the method used, the modified disc diffusion-method, was not able to identify the potential antibacterial effects of CGA and 8b.

The novel drug delivery system showed potential of both eradicating infection and increasing healing, but further testing is needed to assure stability, effective drug release, non-toxic effects on host cells and to characterize the antibacterial activity of CGA and 8b.

Keywords: antimicrobial peptides; chitosan; liposomes; hydrogel; antibacterial resistance; chronic wound healing

Sammendrag

Kroniske sår er en stor belastning, da de forårsaker både sykkelighet og dødelighet hos pasienter, samt en massiv økonomisk belastning på helsevesenet verden over. Disse sårene har høy grad av kompleksitet og er ofte vanskelige å behandle på grunn av de mange faktorene som begrenser sårheling, som betennelse, biofilmdannelse og bakterielle infeksjoner. Med disse typisk vedvarende infeksjonene, sammen med en økende trussel om antibiotikaresistens, er det et presserende behov for nye og effektive dermale antimikrobielle behandlinger. En gruppe av nye antibiotika som har fått fokus de siste årene er antimikrobielle peptider (AMP). Bruk av disse forbindelsene kan være en lovende behandling av hudinfeksjoner, men for kroniske sår er sannsynligheten liten for effektiv terapi gjennom behandling av kun enkeltmål. Målet for prosjektet var derfor å utvikle et nytt dermalt legemiddelleveringssystem som både kan utrydde bakterielle hudinfeksjoner, samt øke tilheling av kroniske sår. Dette ble gjort ved å kombinere klorogensyre (CGA) og en syntetisk etterligning av et antimikrobielt peptid i en liposom-i-hydrogel-formulering med en bioaktiv polymer.

CGA og vår AMP kalt 8b ble både inkorporert hver for seg og sammen i liposomer. Testing av relevante egenskaper ble utført over en 12-ukers periode for å vurdere både stabilitet og leveringssystemets evne til å gi en effektiv og sikker behandling i hud.

Rett etter produksjon hadde liposomene med to virkestoffer en gjennomsnittlig vesikkelstørrelse på $208 \pm 2,5$ nm og en polydispersitetsindeks (PI) på $0,083 \pm 0,017$, et zetapotensial på $40,0 \pm 1,3$ mV og en pH på $3,00 \pm 0,02$. Evnen til innkapsling av aktiv forbindelse var mer effektiv i liposomer med to virkestoff enn for liposomer med et virkestoff, med en innkapslingseffektivitet på 43,5 % for CGA og 80,2 % for AMP 8b. Alle egenskapene til den liposomale suspensjonen viste adekvat stabilitet over de 12 ukene.

De liposomale suspensjonene ble inkorporert i en kitosanhydrogel og karakterisert over en 12 ukers periode. pH lå stabil på omtrent 4,8 under lagringsperioden. Den reologiske testingen viste en pseudoplastisk flyt, egnet for dermal påføring. Måling av teksturegenskaper for liposom-i-hydrogel viste at formuleringene som inkorporerte CGA hadde betydelige endringer i både hardhet og kohesivitet i perioden mellom 4 og 12 uker etter produksjon. Karakterisering av frigjøring fra liposom-i-hydrogel-formuleringen viste en stabil frigjøring av 8b, men en manglende evne til detekterbar frigjøring av CGA. Den antioksidative aktiviteten til CGA ble vurdert og sammenlignet med de velkjente antioksidantene vitamin C og E. Testing av cellulær

kompatibilitet viste en uventet toksisk effekt på murine makrofager for mer høykonsentrerte hydrogeler og formuleringer som inneholdt CGA. Både vanlig kitosanhydrogel og liposom-i-hydrogel-formuleringer viste effektiv hemming av bakterievekst i både gram-positive og gram-negative bakterier, men metoden som ble brukt, en modifisert versjon av diskdiffusjon, var ikke i stand til å identifisere de potensielle antibakterielle effektene til CGA og 8b.

Det nye legemiddelleveringssystemet viste potensial for både utrydding av infeksjon, samt økning i sårheling. Ytterligere testing er nødvendig for å sikre stabilitet, effektiv frigjøring av virkestoffer, ikke-toksiske effekter på vertsceller og for å karakterisere den antibakterielle aktiviteten til CGA og 8b.

Nøkkelord: antimikrobielle peptider; kitosan; liposomer; hydrogel; antibakteriell resistens; tilheling av kroniske sår

1 General introduction

Antibiotic resistance is classified by the World Health Organization (WHO) as one of the biggest threats to human health due to misuse in medicine, food industry and agriculture. Simultaneously, the development of new antibiotics has halted, raising concerns of a future without effective therapeutic options (1;2). Consequently, novel antimicrobial alternatives are urgently needed.

Skin and soft tissue infections (SSTIs) are some of the most common infections and increasing antimicrobial resistance has been reported for topical antibiotics (2). Bacterial skin infections may prevent healing of damaged skin. These non-healing and infected wounds represent a rapidly increasing burden on the health care system (3). A chronic wound is defined as a wound that has not healed spontaneously to normal structure and function within three months (4;5). They can be both painful and put patients at increased risk of potentially life threatening infections (3).

The cause of limited healing in chronic wounds are often multifactorial. The majority of chronic wounds are colonized by bacteria in biofilms, protecting the pathogenic bacteria, making eradication challenging (4). They are also typically locked in a prolonged inflammatory state, delaying healing. Effective treatment through single-targeted therapeutics is unlikely. For successful treatment, combination therapy of effective drugs in a suitable delivery system is required to eliminate both the infection, bacterial biofilm and the persistent inflammation (3).

A promising new strategy for the treatment of SSTIs and chronic wounds are the use of synthetic mimics of antimicrobial peptides (SMAMPs). Antimicrobial peptides (AMPs) are a part of the skin's innate immunity, but the synthetic mimics are more stable, less toxic and have improved pharmacokinetic properties compared to their natural counterparts. The AMPs have a broad-spectrum and rapid antimicrobial effect, low resistance development, as well as immunomodulatory and wound healing properties (2;6). These are all properties that could be beneficial in the treatment of chronic wounds.

The primary challenges hindering the clinical viability of AMPs for dermal application, are their low *in vivo* stability and toxicity. A proposed solution is the incorporation of AMPs in drug carriers such as liposomes (2). Liposomes are small, spherical, lipid vesicles with the ability of encapsulating both lipophilic and hydrophilic compounds. They are often used in

dermal drug delivery where they can improve stability and prolong effect (7;8). Liposomes are made as suspensions and are thus not suited for topical application. To overcome this limitation, use of a primary and second vehicle, such as liposomes in hydrogel, can be applied to ensure appropriate texture properties (9;10). These liposome-in-hydrogel formulations are suitable for delivery of antimicrobial compounds as they have a prolonged and sustained release, limiting the exposure of sub-inhibitory concentrations of drug and need for reapplication of formulation (11;12).

Chitosan is a bioactive polymer used in the production of hydrogels. It has intrinsic antimicrobial, antibiofilm, anti-inflammatory and wound-healing properties, and has the ability to act in synergy with other antimicrobials (1;13;14). This suggests that a chitosan hydrogel with dual-loaded liposomes incorporating antimicrobial and healing-inducing active compounds could be an effective therapeutic option for chronic wounds.

2 Introduction

2.1 Skin

The human body's first line defense is the skin. As the largest organ and outermost barrier, it is exposed to a wide array of threats, both physical injuries and pathogens. As a result, the skin possesses protective and regenerative properties to support the barrier function (12).

The skin itself has a multi-layered structure, divided in three primary layers; epidermis, dermis and hypodermis (Figure 1) (15). The stratum corneum, the top part of the epidermal layer, is the outermost layer of the skin. It provides a physical barrier that prevents microbes from penetrating the skin. The stratum corneum has a "brick and mortar" structure (Figure 2), with corneocytes as bricks surrounded by the mortar, the intracellular lipid matrix. This structure enhances the barrier function of the skin. The stratum corneum has an acidic pH of approximately 5.5, making it an inhospitable environment for bacterial growth. Desquamation, the process where the stratum corneum peels off and completely replaces itself every two to four weeks, further adds to the inhospitality and provides further protective properties (12;16).

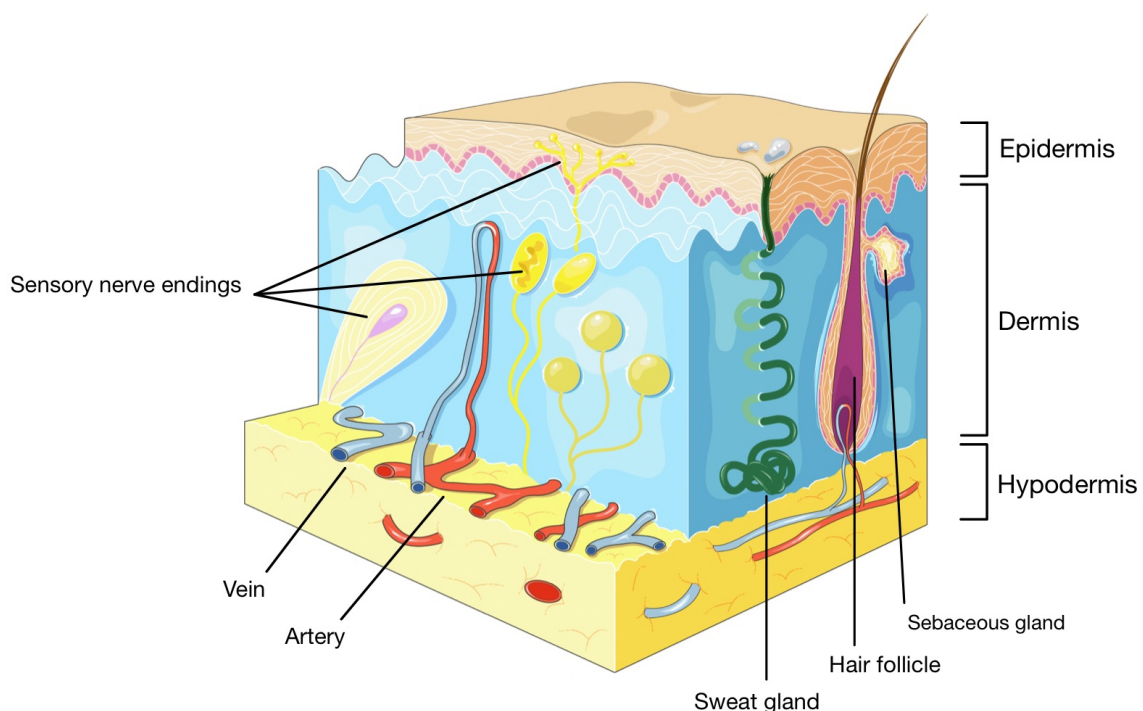


Figure 1: Cross-section of the skin structure, displaying the three skin layers, epidermis, dermis and hypodermis. Several structures, such as blood vessels, sensory nerve endings, hair follicles and sweat- and sebaceous glands, are embedded in the different layers of skin. Illustration element provided by smart.servier.com.

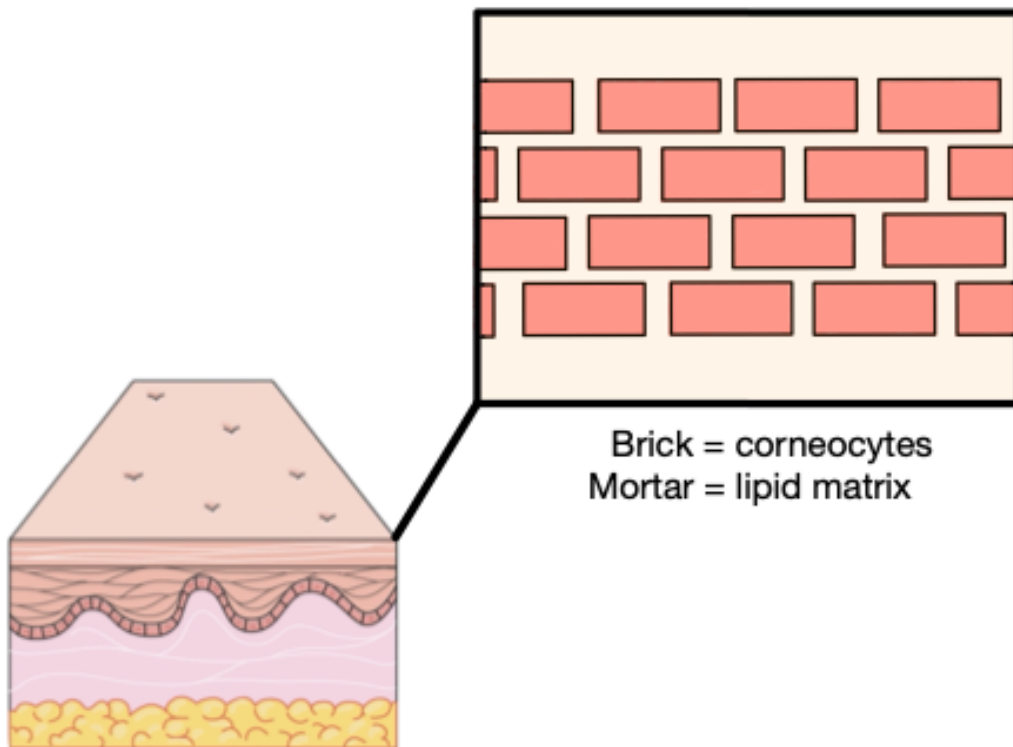


Figure 2: Illustration of the stratum corneum with the brick and mortar model. The stratum corneum is the outermost layer of the epidermis. The bricks represent the corneocytes embedded the mortar, an intracellular lipid matrix. Illustration element provided by smart.servier.com.

In addition to being a physical barrier, the epidermis serves as a residence for a great number of immune cells. If the skin is wounded and the physical barrier breached, a network involving various receptors, immune cells and signaling molecules will protect the deeper tissue from infections by pathogens (2). To support this immune response, cells in the epidermis produce antimicrobial peptides (AMPs) with the ability to inhibit microbial growth both through direct antimicrobial effect and immune and inflammation modulating properties (17). The epidermis skin layer is also inhabited by commensal microorganisms in a microbiome. These bacteria and fungi play a significant role in skin health, as they do not cause infection when in balance with the host's immune system, and may inhibit growth of pathogenic bacteria (12).

As the body's protective barrier, a breach to the skin could serve as an entry point for either microorganisms from skin microbiome or pathogenic bacteria from the environment to deeper skin tissue with more optimal conditions for growth (12;18). The risk of invasive infections, chronic wounds, tissue damage and systemic effects such as sepsis underlines the importance of an intact skin barrier (12).

2.1.1 Wound healing

Because of the significant health risk caused by barrier damage, the skin has strong wound healing properties for restoring tissue integrity. This is a complex process involving a series of events engaging several cells, growth factors and cytokines (3;19). The wound healing process is generally divided into four phases: hemostasis, inflammation, proliferation and remodeling, which are connected and overlapping (Figure 3) (3). The first phase, hemostasis, starts immediately after injury (5). The main goal is to stop loss of blood and provide a fibrin matrix scaffold for cells, cytokines and growth factors needed for further healing. Following closely is the inflammation phase, where a cascade of signaling molecules promotes activity of phagocytic cells, such as neutrophils and macrophages. This process is essential for preventing infection at wound site. Proliferation is the process where an acute wound goes into a repair stage through some extensive healing processes. It occurs within days of the injury and is characterized by formation of granulation tissue (3;5). In the last phase, remodeling, all previous processes cease. This is a longer process where new epithelium and scar tissue is formed and may last for years after injury (5;19).

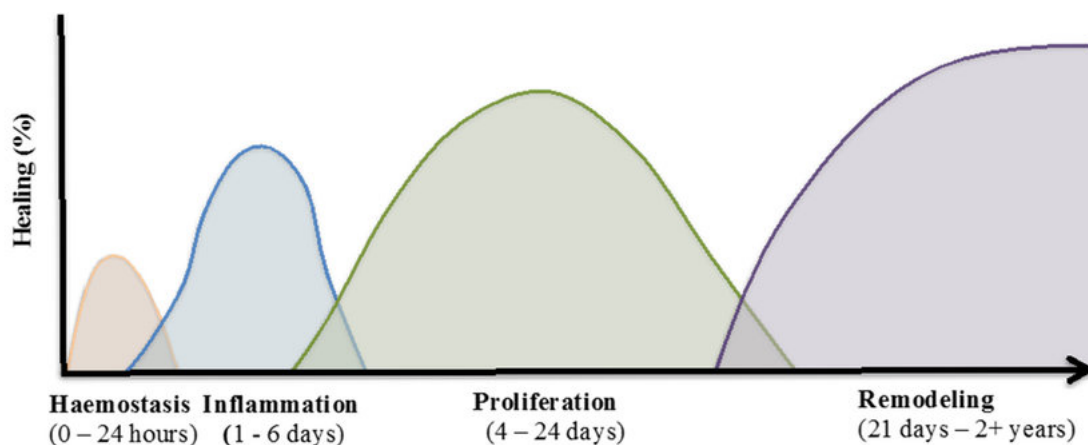


Figure 3: The four continuous and overlapping phases of wound healing; hemostasis, inflammation, proliferation and remodeling. The figure illustrates when the different phases are contributing to healing over the timespan of the healing process (open access, permission granted) (20).

Normal cutaneous healing is characterized by an organized and tightly regulated cascade of events (12;18). The wound should be clean, have healthy granulation tissue and a growing epidermal edge (4). Failure to move through the repair process in a normal manner can cause

chronification of the wound (12;19). This results in a deficient skin barrier with suboptimal anatomical and functional integrity (19).

2.2 Chronic wounds

After skin damage, the body initiates wound healing. Failure to move through the wound healing phases results in a non-healing chronic wound (3). A chronic wound is defined as a wound that has not healed spontaneously to normal structure and function within three months (4;5). Most fall into the categories of arterial, venous, pressure or diabetic ulcers (3;4).

Complications caused by wounds result in both morbidity and mortality (5). A non-healing wound is a big burden, both on the patient and the health care system as a whole. They represent a massive economical strain on health care systems worldwide, and with an increasing prevalence of patients with risk factors, such as old age, diabetes and obesity, the cost is only expected to rise (1;3-5;18). Chronic wounds cause both pain and loss of function. Patients are also exposed to an increased risk of infection that may lead to potential amputations or sepsis (3). Even with the high prevalence and cost of care, efficient treatment for chronic wounds is lacking (18). There is an unmet clinical need for new therapies, and research into causes of chronic wounds and efficient wound management is urgently needed (3-5).

2.2.1 Inflammation in chronic wounds

When a wound fails to heal, it is detained in a continuous inflammation stage (3). The inflammatory phase of wound healing is supposed to act as an immune barrier against pathogenic bacteria (5;12). Locked in a prolonged and heightened inflammatory state, the wound is characterized by a high number of neutrophils, reactive oxygen species (ROS) and destructive enzymes. There is a fine balance between pro-inflammatory signaling molecules and their inhibitors. If this balance is disrupted, wound healing could fail (3). Extensive inflammation is a big contributor to a failed healing cascade by delaying proliferation and epithelization (1;3). The ultimate aim would be to eliminate the persistent inflammation cycle delaying wound healing for a more effective treatment (3).

Other factors such as low blood supply, trauma and bacterial infections can also prevent healing progression. A local decreased blood supply is associated with the inflammatory state

disrupting wound healing, and many chronic wounds occur for this reason. Additionally, the balance between ROS and antioxidants is also disrupted in chronic wounds (3).

2.2.2 Infections in chronic wounds

Chronic wounds are an easy access opening to the body and are often infected by microorganisms. The colonizing bacteria can either be from the environment or the body's own microbiota (18). Fungal infections usually happens at a later stage than bacterial infections (12). Wounds serve as entry ways for microorganisms to the deeper skin tissues, where they have more optimal conditions for colonization and growth (18). A breach to the skin barrier can also alter the surface pH. Chronic wounds are typically neutral to alkaline. A change from the natural acidic conditions on the stratum corneum could be more advantageous for bacteria (1;12). After colonization, the bacteria negatively affect wound healing through immune stimulation and virulence factors. To enable healing, the bacteria levels must be reduced (12;18;19).

Chronic wounds are often polymicrobial, infected by more than one bacterium, making eradication hard (3;4). Most frequent bacteria found in skin infections are *Staphylococcus aureus*, *Pseudomonas aeruginosa* and *Escherichia coli* (1;2). A big challenge for antimicrobial skin therapy is the wide variety of bacteria and diversity between patients (1).

Antibiotic resistance is also a concern, classified by the World Health Organization (WHO) as one of the biggest threats to human health due to misuse in medicine, food industry and agriculture (1;2). This is also the case in wound therapy, with resistant bacteria such as methicillin resistant *S. aureus* (MRSA) causing many infections (21). In addition, multi-drug resistant bacteria are rising threats (22). This, in combination with the polymicrobial biofilms typical for bacterial skin infections, underlines the importance of novel strategies to be able to eradicate bacteria and promote wound healing (23).

2.2.3 Treatment of chronic wounds

Treatment of chronic wounds is generally focused on limiting the factors that inhibit spontaneous wound healing (19). Some of the most prominent challenges are polymicrobial infections, antimicrobial resistance, biofilms, altered pH, inflammation, restricted blood flow and being unable to achieve sufficient local antimicrobial concentration (12). In antimicrobial

treatment, choice of antibiotic is based on the infectious bacteria (1). Effective treatment through single target therapeutic is unlikely, as both bacterial eradication and promotion of healing is necessary for wound healing (3;18).

Treatment can be administered both topically and systemically (12). Use of topical formulations is not uncommon, but the scientific evidence behind the use is limited. Wounds emit fluids through exudation to maintain a moist wound bed and help the healing cascade. Larger volumes of exudate can cause problems for retention and residence time of local therapeutics (1). Repeated application and spreading of creams and ointments in wounds can be painful and damage the wound area, creating further setbacks for wound healing. Additionally, open wounds require sterile formulations (1;12). The general complexity of wounds is a barrier for clinical use of novel pharmaceutical formulations. Research and scientific advances are necessary for developing new and effective treatment (3).

2.3 Biofilms

A considerable issue in the treatment of skin wounds are bacterial biofilms (2). Even though antibiotic resistance in bacteria is a result of genetic mutations, biofilm formation is considered an important resistance mechanism of some pathogenic bacteria (13;23). In the past, the influence of biofilms on wound healing has been underestimated and only recently gained wider recognition (24). Infections involving biofilm formation cause more damage and greater inflammatory responses than infections by planktonic bacteria (25). Biofilm-associated diseases are costly for the health care system, and with increasing life expectancy and number of people with chronic medical conditions, this cost is only expected to rise (4;25). Despite this, there is a lack of sufficient research on new antibiotic drugs, largely due to the difficulty and expenses associated with discovery of new treatment strategies. Additionally, most of the current antimicrobial research is focused on effects on planktonic bacteria, even though bacteria causing skin infections predominantly exist within biofilms (25).

Biofilms are structural polymeric aggregates composed of extracellular polysaccharides, glycolipids, extracellular DNA and proteins that grant adhesive and protective properties (4;13). Formation of biofilms starts when planktonic bacteria overcome the electrostatic repulsive forces between the bacterial cell surface and substratum and attaches to the skin. When the rapid biofilm formation starts, the bacteria achieve protection and new characteristics,

like an increased resistance to antimicrobial compounds and host immunity (Figure 4). Biofilms can adhere strongly to the skin and penetrate to deeper skin layers, making the eradication and treatment of biofilm infections challenging (1;24;25).

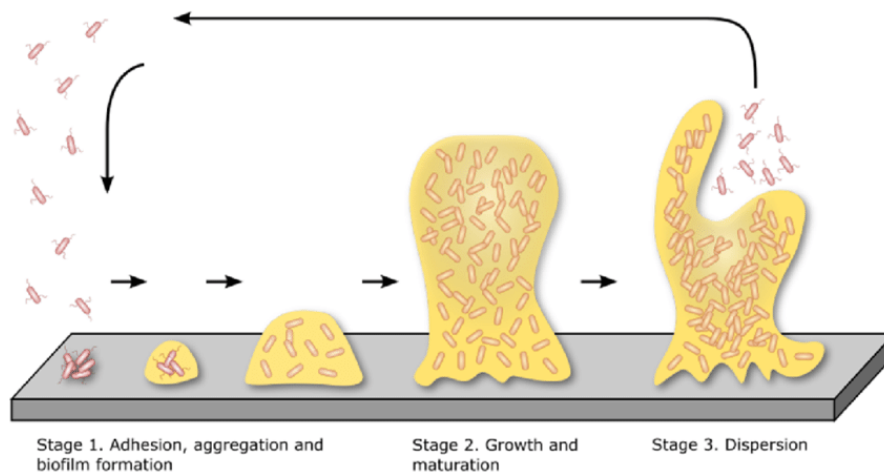


Figure 4: Stages in biofilm formation. (1) Free planktonic bacteria adhere to surface, forming the biofilm. (2) Growth and maturation of the biofilm. The polymeric substances grant improved adhesion and protection, making eradication challenging. (3) Free bacteria are released from the biofilm to continue colonization (open access, permission granted) (26).

The majority of human chronic wounds, about 60-80%, are colonized by bacteria in a biofilm (4;25). These biofilms are often polymicrobial with typically 12-20 different species, though higher numbers are not uncommon (4). Chronic wounds show considerable heterogeneity, where pathogenic bacteria becoming predominant at the expense of commensal species (25). This may be the reason why polymicrobial biofilms are shown to have higher virulence than single-species biofilms. The most common bacteria to generate biofilms are *S. aureus*, commonly situated more superficially, and *P. aeruginosa*, typically located deeper in the wound (4).

Infections resulting from the formation of biofilms are notoriously hard to eradicate (4;25). This is because biofilms are recalcitrant to elimination by both the hosts immune system and antimicrobial agents. Biofilms hide the pathogenic bacteria from the immune system. This makes leukocytes and macrophages unable to eradicate infection, generating a state of chronic tissue inflammation (4). This persistent inflammatory state is linked to damaged tissue and reduced wound healing (12;24).

Compared to free swimming cells, bacteria in biofilms have 100-1000 times decreased susceptibility to antimicrobial treatments. The lack of effectiveness is mostly due to limited penetration of antibiotics through the biofilm, and results in a more challenging therapy (2;25). Inadequate perfusion may culminate in not being able to meet minimal inhibitory concentration (MIC) (4). A limitation of oxygen and nutrients in the biofilm also decrease the metabolic rate of biofilm bacteria, putting them in a dormant state. This makes antibiotics that targets cell division less effective (1;12). The practice of antibiotics being prescribed based on MIC, which measures the action of antibiotics on planktonic bacteria in acute infections, often renders treatment of chronic infections involving biofilm based on MIC ineffective (25).

A promising approach to combat biofilm formation is to combine of two different drugs for synergistic effect (13). In this project, both a synthetic mimic of an AMP (SMAMP) and chlorogenic acid (CGA) was incorporated into a liposomal hydrogel to hopefully enhance antimicrobial activity.

3 Active compounds

3.1 Antimicrobial peptides

Antimicrobial peptides (AMPs) are amphipathic peptides with innate antibacterial effect (19;27). These substances are an important part of the innate immune system in nearly all living organisms and prevent infections with their antimicrobial activity against bacteria, fungi, viruses and parasites (2;6). In all stages of wound healing, AMPs are upregulated. Not only do most of them possess direct, rapid and broad-spectrum antimicrobial effect, but they are also able to control immune responses, often dysregulated in infected skin, making them an attractive alternative for treatment for chronic wounds (2).

Most natural AMPs are small peptides with somewhere between 12-50 amino acids and a positive net charge. This charge, and the difference in membrane composition between prokaryote and eukaryote cells, enables selective electrostatic interaction with the slightly anionic bacterial membranes (2;28). The AMPs have a rapid bactericidal effect and broad-spectrum activity (27). In contact with bacterial membranes, AMPs have the ability to fold into an amphiphilic conformation important for their mechanism of action. The peptides can insert themselves into the lipid membrane, resulting in formation of transmembrane pores or membrane disruption. Even though the mechanism of membrane interactions is not fully

understood, multiple models have been proposed (Figure 5). In the barrel pore model, several AMPs form a barrel-shaped complex and insert themselves into the membrane, with their hydrophilic region facing the center of the pore. The toroidal pore model is similar to the barrel pore model but assume interaction with the head groups of the cell membrane phospholipids. In the carpet model, the hydrophobic parts of AMPs attach to and coat some areas membrane, resulting in pore formation (29). Non-membrane disruptive peptides can also interfere with intracellular targets, affecting enzymes and synthesis of cell wall, nucleic acid and proteins (2).

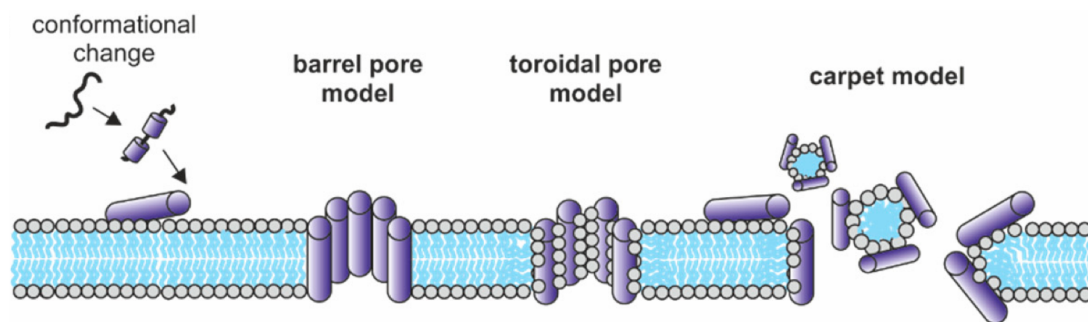


Figure 5: Proposed mechanisms of membrane interaction between AMPs and bacterial cell membrane. The prior conformational change is essential for the suggested mechanisms (open access, permission granted) (30).

Application and clinical use of natural AMPs are limited by their toxicity, instability, pharmacokinetic properties and high production costs. Design of SMAMPs based on the pharmacophore model of small AMPs could offer a solution to these limitations (2;27).

With the skin being an effective barrier for drug penetration, topical administration of AMPs requires sufficient tissue penetration for effective antimicrobial treatment. The AMPs are prone to degradation and the lack of *in vivo* stability can limit their clinical relevance. Both skin penetration and stability in the proximity of skin enzymes should be examined when considering an AMP or SMAMP for clinical use. Measures to increase topical bioavailability could be to encapsulate the drug in a drug delivery system such as a hydrophobic nanoparticle carrier (2;27). Clinical relevance could also be increased by the carriers ability to reduce toxicity and prevent potential harmful side effects (31).

The SMAMP utilized in this project is a synthetic amphipathic barbiturate, described by Paulsen *et al.* (6). These structures are inspired by the pharmacophore model of small AMPs

and the marine antimicrobials eusynstyleamides isolated from the marine Arctic bryozoan *Tegella cf. spitzbergensis* and the Australian ascidian *Eusyntyela lactericus*, a chiral barbiturate scaffold with two cationic groups and two lipophilic side chains. These structures showed an immediate and strong membrane disrupting effect, supporting that the approach could be used in the design of SMAMPs against multi-resistant bacteria (6).

3.2 Chlorogenic acid

Wound healing is a multifactorial physiological process, so a single-targeted approach such as lowering immune response or targeting a single cellular constituent, will likely offer limited success. To expect clinical efficacy of a novel drug delivery formulation against skin and soft tissue infections (SSTIs), we need a multi-targeted approach that modulates components of tissue regeneration and confine factors limiting wound healing (32).

Many different factors can present a risk for delaying wound healing, such as bacterial infections or over-production of ROS. Using antioxidative and antibacterial compounds, such as CGA, may improve wound healing (32).

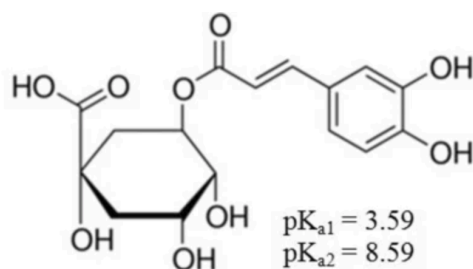


Figure 6: Chemical structure of chlorogenic acid including pK_a values for the carboxyl group and first phenolic group (open access, permission granted) (33).

Chlorogenic acid is a polyphenol and secondary plant metabolite that has shown among other antibacterial, antioxidative and antiphlogistic activity. It displays an antibacterial effect in both gram-positive and gram-negative bacteria (32;34;35). The mechanism of chlorogenic acid's antibacterial effect is the ability to bind and permeabilize the cell membrane. In research, chlorogenic acid killed pathogenic bacteria strains of *Shigella dysenteriae* and *Streptococcus pneumoniae* by provoking irreversible permeability changes in the cell membrane. This caused the bacterial cells to lose the ability to maintain membrane potential and cytoplasm

macromolecules, including nucleotides (35). Its effect on the cell membrane was also shown to effectively inhibit growth of *S. aureus*, an important bacteria causing skin infections with an increasing antimicrobial resistance (34). CGA is known to have a minimal toxicity level (36). In a study by Moghadam *et al.*, no toxicity was observed in keratinocytes, fibroblast or endothelial cells. Enhancement of keratinocyte wound closure and capillary-tube formation in endothelial cells was also observed (32).

In this project we aimed to incorporate CGA into our liposomes for a synergetic effect with our SMAMP. As a polyphenolic acid, CGA is soluble in water and will therefore be incorporated into the aqueous phase of the liposomes, while the AMP will be incorporated in the lipophilic phase (32).

4 Drug delivery system

4.1 Dermal drug delivery

Local dermal therapy is considered an attractive administration route for antimicrobial compounds or chronic wounds and a good alternative to oral administration. Systemic antibiotics for wound infections require a high serum level to reach a therapeutic concentration in skin tissue, resulting in more adverse effects (12). Local administered drugs have the ability to diffuse into surrounding tissue, achieving higher local drug concentrations, while avoiding systemic absorption and higher potential for side effects (1;16). Other advantageous factors are the possibility of sustained drug release, lower fluctuations in drug levels, avoidance of first-pass metabolism and improved patient compliance (37).

For both dermal and transdermal drug delivery, the biggest barrier is the stratum corneum of the outer epidermal layer, impairing penetration and absorption. The barrier function of skin may be impaired due to physical state or inflammation, resulting in different drug absorption compared to healthy skin. In wound therapy, the physical state of the skin can alter drug effect and an open wound can increase penetration and absorption across the skin (1;37).

The interaction between the skin and a drug delivery system, and the following mechanism of drug release is not fully described. The penetration through skin is driven by passive diffusion by the concentration gradient (16). Four different mechanisms of drug release from lipid vesicles to skin have been presented. The first proposed mechanism is the penetration of intact

vesicles. The relevance of this mechanism has been up for debate in the scientific community (37;38). Second is that lipid vesicles, with their skin fluidizing properties, work as penetration enhancers. Third mechanism is carrier-skin drug exchange, a direct transfer of drug in lipid bilayer and surface of stratum corneum. The fourth and last suggested mechanism is transdermal drug delivery through hair follicles and sweat ducts (37).

In local dermal therapy, successful treatment is dependent on drug penetration deep enough to reach therapeutic site while avoiding absorption to systemic circulation (1). The blood vessels necessary to reach for transdermal effect are located in the dermis, and deep penetration of drug, or penetration through the transfollicular route can therefore result in systemic effect and lower local effect (8;15). How the drug is delivered to the skin is in dependent on the formulation, and in particular the size of the drug carriers (37).

4.2 Liposomes

Liposomes are small, spherical vesicles composed of one or more phospholipid bilayers enclosing an aqueous core. Their size can range from 30 nm to several micrometers (7;16). Liposomes are prepared as suspensions via various methods. In this project we utilized the thin film method, involving rehydration of a dry lipid film in aqueous solution, self-assembling spontaneously, forming a closed structure. Phospholipids are composed of a polar head group and two hydrophobic chains (Figure 7). The head group face towards the medium and core, influencing the surface properties. The hydrocarbon chains, making up the bilayer, can have different lengths and degrees of unsaturation, affecting the fluidity of the liposomal membrane (7;31;39).

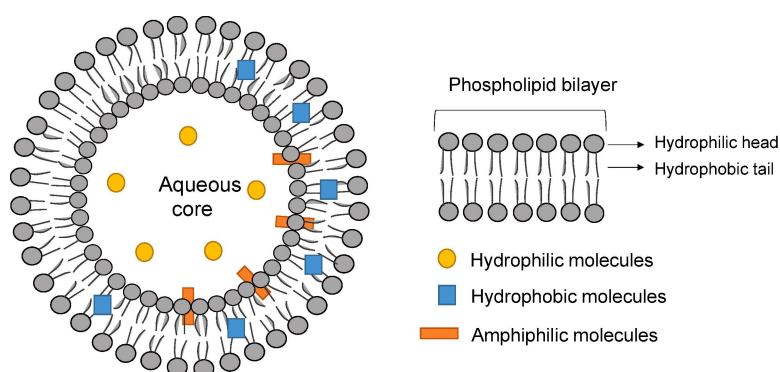


Figure 7: General structure of unilamellar liposome showing the arrangement of phospholipid bilayer. Location of incorporated molecules, such as active compounds, is dependent on their hydrophilicity or lipophilicity, and consequently the ability to solubilize in the liposomal region of question (with permission) (40).

Active compounds, such as antibiotics, can be loaded into liposomes, protecting them from deactivation and reducing toxicity (31). Liposomes have the ability to encapsulate both lipophilic and hydrophilic compounds (8;9). Lipophilic and amphiphilic drugs can be contained in the lipid bilayer, while hydrophilic drugs are present in the aqueous core (7;16). The loading capacity of liposomes are relatively high, and the number of antimicrobial drugs suitable for liposomal entrapment is large (31).

Lipid-based carriers, such as liposomes, are extensively used as drug carriers for skin delivery due to their many advantages. They are biodegradable, biocompatible and non-toxic, can increase the bioavailability of poorly soluble drugs and protect entrapped drug, resulting in improved stability and a prolonged and enhanced effect (8-10;37;41).

Liposomes are commonly used to promote the of efficacy for current antimicrobial drugs (10;16;31). Drugs entrapped in liposomes have enhanced efficacy and reduced toxicity compared to free drug (7). Many antibiotics that are ineffective in free solution due to bacterial resistance in either gram-positive or gram-negative bacteria, have been demonstrated to be effective antibacterial drugs when encapsulated in liposomes with size in the nano-range. Some of this may be contributed to the protection from enzymatic deactivation and fusogenicity of liposomes. Fusogenicity is contributed to their phospholipid bilayer structure resembling the bacterial cell membranes. This similarity gives liposomes as drug carriers an additional ability to fuse with the outer membrane of bacterial cells and promote intracellular drug release (31).

4.2.1 Effect of liposomal size on nanoscale

Liposomal size is a critical attribute, affecting safety, stability and efficacy, both *in vitro* and *in vivo*, but due to the small scale, determining the exact size of nanoparticles can be challenging. Size is often stated as a mean value, influenced by its mode of distribution and size weighting. The size must therefore be seen as a result of its measuring technique (8).

As a result of its synthesis, liposomes have inherent polydispersity, meaning a distribution of different sizes and shapes in the same batch. Polydispersity index (PI) describes the degree of non-uniformity of a size distribution within a sample. A value for 0.0 describes a perfectly monodispersed system, while a highly polydispersed system would get a value closer to 1.0 (8). For lipid-based carriers, such as liposomes, often used in dermal drug delivery, a PI under 0.3 is deemed acceptable (8;16).

The use of nanoscale particles offers new technological opportunities in the drug-delivery field (42). The established nano-size range is often considered as 1 to 100 nm, but nanoparticles can comprise the whole nano-range, with particle sizes up to 1000 nm (43-45). With all the challenges in chronic wound therapy, such as infections, biofilm, inflammation, multi-drug resistant bacteria, it could be a compelling opportunity to utilize the innovation in the nanomedicine field (22). Nanotechnology has been used to develop novel topical drug delivery systems facilitating drug delivery over the skin barrier (37;46). Many of these have an aim of treating wounds and infectious biofilms (12;31). Size is a critical property in skin delivery, and both permeation and state of skin should be considered when choosing drug carrier size. Optimal liposomal size for dermal drug delivery is suggested to be between 200-300 nm, with liposomes of 300 nm showing a higher reservoir and drug concentration in all skin layers, compared to 60 nm and 600 nm (38;41). The determination of drug concentration in the different skin layers is challenging, and more research on dermal drug delivery is still needed (1;38).

Biofilms are significant barriers for antimicrobial therapy in skin infections (1). Particles smaller than 350 nm have the ability to diffuse through pores in the biofilm. This may enable delivery of antimicrobial drugs in the biofilm. The sustained release from nanoparticles also enables prolonged exposure to effective levels of antibiotics, enhancing the effect on slow growing bacteria in biofilms (22).

4.2.2 Effect of liposomal charge

Stability of liposomal suspensions are influenced by their zeta potential (ZP), determined by the head group of the phospholipids that forge the liposomes. A zeta potential between -10 mV and 10 mV is considered neutral. Liposomal suspensions typically require a charge above 30 mV or below -30 mV to have the necessary electrostatic repulsion to be considered stable. By preventing instability of the liposomal bilayer structure, the liposomes are less likely to have drug leakage and aggregation. This preserves the homogeneity of the drug delivery system (10;31;39). The ZP is affected by pH, ionic strength and particle concentration, but the biggest influence on the surface charge of liposomes is the phospholipid composition (39).

Charged liposomes could be attractive for wound therapy. With cationic drug delivery systems, electrostatic attraction is stronger with anionic bacterial membranes compared to neutral

mammalian cell membranes. This is an advantage in topical antimicrobial therapy by improving both efficacy and safety (10;31).

4.3 Hydrogel

Hydrogels are semisolid formulations made of hydrophilic polymers in water. The physical and chemical crosslinks between the polymers forms a three-dimensional network that is insoluble in water. Hydrophilic groups on the polymer chains give the hydrogel a high hydrophilicity and ability to absorb water. Due to their high water content, hydrogels are soft and pliable (12;14). Their flexibility makes them suitable for appliance on damaged skin, as they form to the wound area and mechanical damage during appliance is minimized (11;12).

The high water content also gives hydrogels wound healing properties. While covering and protecting the wound, the hydrogel also provides a moist wound environment, absorbs excess wound exudate, and provides high oxygen permeability for accelerated healing (11;12). A moist wound environment can on the contrary affect the properties of the topically applied gel. The drug delivery system has the ability to absorb fluid, influencing its mobility, local adhesion and drug delivery rate (12;19).

The pH of hydrogels can affect wound healing. Unimpaired human skin has a pH between 4 and 6, while wounded skin typically have a higher pH. This suggests that a more acidic hydrogel could help restoring a lower pH environment and facilitate wound healing (10). Other hydrogel properties important for topical administration, such as viscosity and texture properties, depend on the composition of the hydrogel and can therefore be modified (11).

4.3.1 Chitosan in hydrogel

Chitosan is one of the most promising and frequently used biomaterial ingredient in hydrogel preparation (1;10). It is a nature-derived polymer from the partial alkaline deacetylation of its parent polymer chitin. Chitin is abundant in nature, where the main sources are shell waste of shrimps, lobsters, krill and crabs. Chitosan is derived from natural sources and has been shown to have excellent biocompatibility and biodegradability. The polymer is shown to be non-toxic, non-allergenic and ecologically safe, and with intrinsic antimicrobial, antibiofilm and wound-

healing properties, chitosan is considered as being an effective biomaterial with a wide range of applications. (13;14)

Chitins poor solubility in aqueous solutions and organic solvents consequently results in no practical application whereas chitosan has a wide range of application. This is because chitosan is readily water soluble in acidic solutions (14). Chitosan is a polysaccharide consisting of two monosaccharides: D-glucosamine and N-acetyl glucosamine (13). After deacetylation, the amine groups of chitosan have a pKa value between 6 and 6.5, making chitosan a water-soluble cationic polyelectrolyte in acid solutions under pH 6 due to the protonation of the amine group. The pKa value is highly dependent on the degree of deacetylation (DD) and molecular weight (Mw), and therefore the method of deacetylation is greatly important for the solubility of chitosan (14).

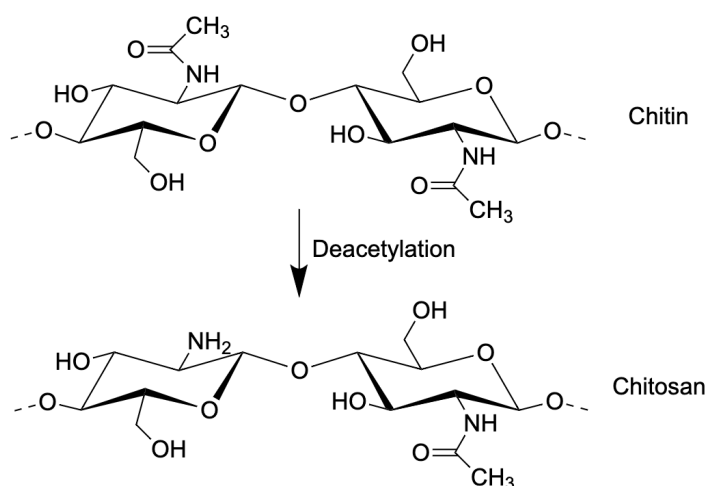


Figure 8: Chemical structure of chitin and chitosan. Chitosan is shown as partially deacetylated, and consists of both D-glucosamine and N-acetyl-glucosamine. Degree of deacetylation and molecular weight of the chitosan polymer can vary depending on the conditions used for deacetylation (14). Created with chemdrawdirect.perkinelmer.cloud.

Hydrogels are composed of a three-dimensional polymer network. Chitosan as a natural bioadhesive polymer, either form a physically associated or chemical cross-linked network to form a hydrogel. In acidic environments, chitosan is an excellent viscosity enhancing agent where the viscosity increases with the concentration. It makes hydrogels behave as a pseudoplastic material demonstrating a decrease in viscosity with increased shear rate. The viscosity of chitosan increases with decreasing temperatures and increasing DD (14). The properties of hydrogels are also affected by the Mw of chitosan. Use of a high Mw chitosan gives a more rigid hydrogel because of its ability to have more cross-linkages per polymer (9).

A chitosan hydrogel has the potential to be antimicrobial, anti-inflammatory, inhibit biofilm formation and have wound healing properties (13;47). Chitosan and its derivatives have the ability to inhibit biofilm formation by an extensive span of bacteria. The ionic interaction between chitosans positively charged amino group and the negatively charged constituents of both the biofilm matrix itself and cell membrane of bacteria, results in impairment of biofilm function and change in cell membrane permeability, with possible DNA complexation, leading to cell death (1;13). Chitosan with higher Mw and DD is often more strongly associated with activity on the bacterial membrane and demonstrate superior wound healing properties (1;23;41). The importance of cationic charge on the effect of chitosan and its derivatives signifies the importance of acidic conditions (1;13).

The anti-inflammatory effect of chitosan comes as a result of its ability to regulate the activity of inflammatory cells and factors under the inflammatory phase of wound healing (47). A liposome-in-hydrogel formulation containing the same concentration of chitosan as in this project, but another entrapped membrane-active antimicrobial compound, has shown anti-inflammatory effect on murine macrophages (23). Chitosan's ability to increase wound healing seems to be a consequence of enhanced vascularization, improvement of the stability of the extracellular matrix and promotion of gas exchange (14;41).

The chitosan hydrogel's ability to electrostatically interact with the cell membrane and biofilm matrix can be further enhance by conjugation of chitosan and cationic AMPs, which inhibit the growth of a broad range of gram-positive and gram-negative bacteria (1;13). With the synergetic effect of the hydrogel formulation and the antimicrobial compound, one could achieve the same effect with a lower drug concentration. This, and the providence of a different antimicrobial mechanism, could lead to lower toxicity and reduce development of antimicrobial resistance (12). The combined drug delivery system could therefore be presented as a safe and effective treatment of skin infections.

4.3.2 Liposomes-in-hydrogel

Liposomes-in-hydrogel (Figure 9) is a suitable formulation for topical drug delivery. The combination of the two delivery systems helps to overcome the shortcomings of each formulation. A suspension of liposomes in an aqueous media is not applicable for direct topical application due to suboptimal viscosity, applicability, spreadability and retention on skin (9;10).

A plain hydrogel formulation is neither suitable as a topical drug delivery system for wound therapy due to fast release from the hydrogel network (1). Additionally, because of their hydrophilicity, hydrogels are predominantly used as vehicles for hydrophilic drugs (9).

To overcome these limitations, use of a primary and second vehicle, such as liposomes in hydrogel, can be applied (9;10). Compared to a plain hydrogel, the inclusion of liposomes enables incorporation of both lipophilic and hydrophilic drugs and improves the release profile of the drug delivery system (1;9). A prolonged release profile of an antimicrobial is desirable due to the possibility of a more predictable and sustained delivery and as a result, limited exposure of sub-inhibitory concentrations of drug (11;12).

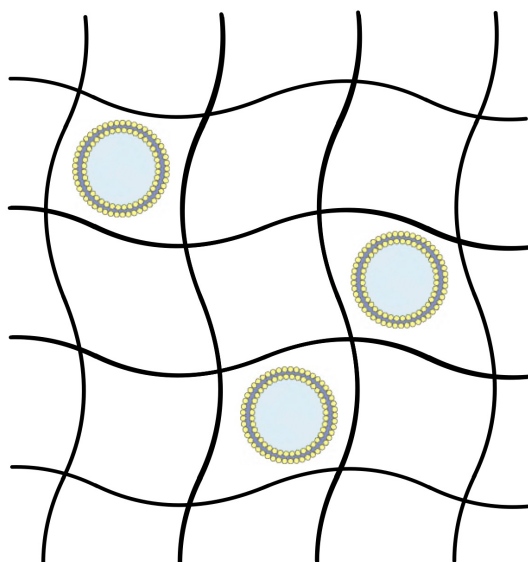


Figure 9: Liposome-in-hydrogel network as a primary and secondary vehicle for effective drug delivery. Illustration element provided by smart.servier.com.

4.3.3 Texture properties of hydrogel

When tailoring a topical drug delivery system, optimizing texture properties is important both for the effectiveness and user-friendliness. The time of contact between formulation and skin is of essence for therapeutic outcome, and the aim is therefore to develop a stable delivery system able to prolong contact. For this, there is a need to control the mechanical properties such as spreadability, applicability, bioadhesion for prolonged contact, an acceptable viscosity and predictable release of active substance (11).

To characterize and optimize the formulation in a simple and reproducible manner, texture analysis can be used. A texture analyser with its moveable probe is able to measure the compressing force when the probe is submerged into a gel formulation and when it returns to its starting point. The plot of the continuous compression force can provide information on the formulation's texture properties affecting wound therapy, such as hardness, cohesiveness, and adhesiveness. With this information, one could monitor the stability or compare different formulations (11).

The mechanical texture properties hardness, cohesiveness and adhesiveness provides much information about how the formulation will behave during use (Figure 10). Hardness is defined as the maximum compressing force applied to the gel and affects the applicability of the gel to the skin. Cohesiveness is the work required to deform the hydrogel in the down movement of the probe. This is displayed as the positive area under the curve in a force-time plot. Lastly, adhesiveness is the work required to redraw the probe. This is displayed as the negative area under the curve of the force-time-plot. This gives an indicator of the retention time on the site of application (11).

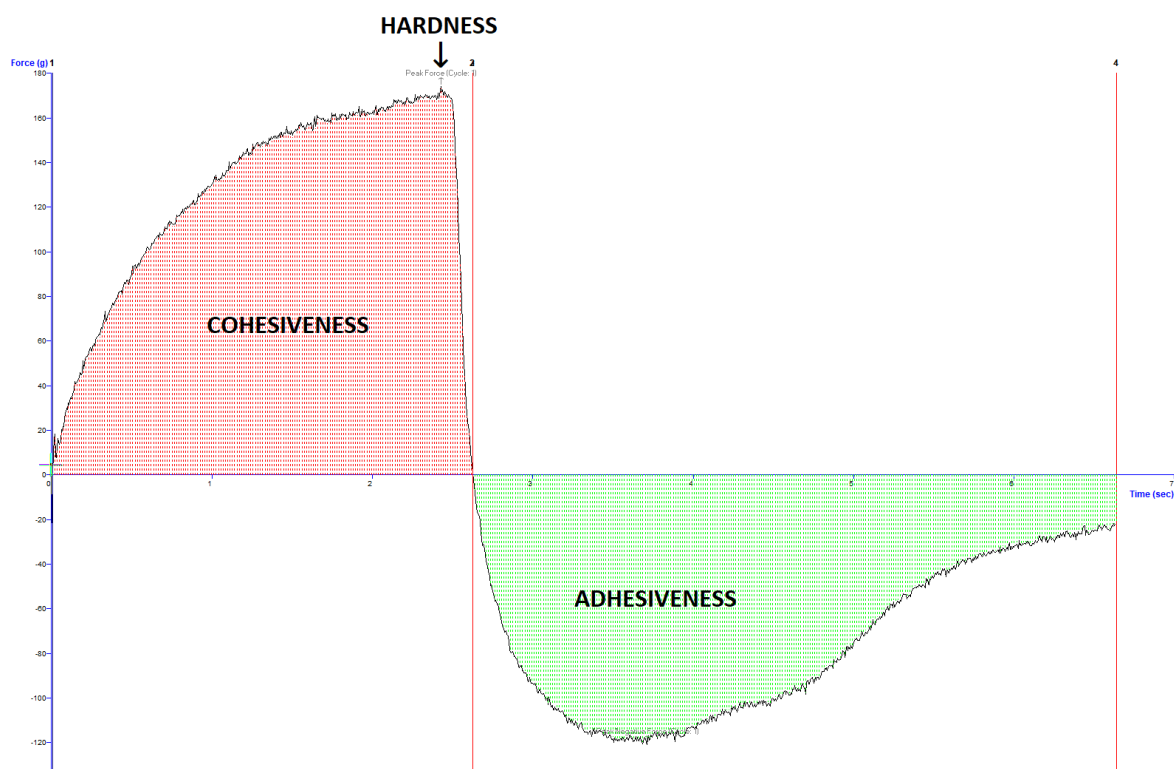


Figure 10: Texture properties on a force-time plot from the texture analysis of arbitrary chitosan hydrogel. The x-axis represents time, the y-axis force. The peak positive force, hardness, represents maximum compression force. Positive area under the curve is cohesiveness and negative area under the curve is adhesiveness.

Gel texture properties are known to depend on the composition of hydrogels (11). To improve the long-term texture properties and the level of deformation or cohesiveness, glycerol was added to the liposomal chitosan-hydrogel (23). In chitosan-based hydrogel, glycerol acts as a stabilizing agent and can slightly reduce the gel cohesiveness (11).

5 Aim of the study

The aim of this project was to develop and evaluate a drug delivery system for increased bacterial eradication and improved wound therapy. A liposome-in-hydrogel formulation including two active compounds and a bioactive polymer was characterized and tested for relevant chemical, physical and biological properties. The proposed formulation should increase activity while reducing toxicity with the intent of improving wound healing and targeting multi-resistant and biofilm-embedded bacteria in both wounds as well as skin and soft tissue infections.

Specific aims for this project:

- Tailor and characterize the liposomal formulation with respect to size, zeta potential, pH, and entrapment efficiency
- Tailor and characterize liposome-in-hydrogel formulation with respect to pH, viscosity, and texture properties
- Evaluate stability of liposome and hydrogel formulation in storage up to 12 weeks after production
- Determine anti-oxidative effects of CGA compared to other conventional antioxidants
- Evaluate antimicrobial effect of this novel formulation on relevant bacterial strains
- Evaluate cell compatibility through toxicological testing on murine macrophages
- Determine drug release through an *in vitro* release study

6 Materials

6.1 Materials

2,2-Azino-bis(3-ethylbenzothiazoline-6-sulfonic acid) diammonium salt, Sigma-Aldrich, St. Louis, Missouri, USA

Acetic acid glacial, AnalaR NORMAPUR®, VWR International, Radnor, Pennsylvania, USA

Acetonitrile HiPerSolv CHROMANORM®, VWR International, Radnor, Pennsylvania, USA

β -cyclodextrin $\geq 97\%$, Sigma-Aldrich, St. Louis, Missouri, USA

Blood agar plates, University Hospital of North Norway, Tromsø, Norway

Cell Counting Kit – 8, Sigma-Aldrich, St. Louis, Missouri, USA

Chitopharm™ M – Medium MW chitosan from shrimp (average of 350-600 kD, $>70\%$ degree of deacetylation), Chitinor AS, Tromsø, Norway

Chloramphenicol $\geq 98\%$, Sigma-Aldrich, St. Louis, Missouri, USA

Chlorogenic acid $\geq 95\%$ titration, Sigma-Aldrich, St. Louis, Missouri, USA

DL-alpha-Tocopherol, Fluka Analytical, Sigma-Aldrich, St. Louis, Missouri, USA

2,2-diphenyl-1-picrylhydrazyl, Sigma-Aldrich, St. Louis, Missouri, USA

Ethanol 96% (v/v) AnalaR NORMAPUR®, VWR International, Radnor, Pennsylvania, USA

Fetal bovine serum, Biowest, Nuaille, France

Glycerol 86%, VWR International, Radnor, Pennsylvania, USA

L-ascorbic acid, Sigma-Aldrich, St. Louis, Missouri, USA

Lipoid S100 ($>94\%$ phosphatidylcholine), Lipoid GmbH, Ludwigshafen, Germany

Methanol AnalaR NORMAPUR®, VWR International, Radnor, Pennsylvania, USA

Methanol HiPerSolv CHROMANORM®, VWR International, Radnor, Pennsylvania, USA

Mueller-Hinton agar plates, University Hospital of North Norway, Tromsø, Norway

Penicillin-Streptomycin (10,000U/mL penicillin, 10mg/mL streptomycin), Sigma-Aldrich, St. Louis, Missouri, USA

Potassium peroxodisulfate, Sigma-Aldrich, St. Louis, Missouri, USA

Roswell Park Memorial Institute (RPMI) medium 1640 with L-glutamine and sodium bicarbonate, liquid, Sigma-Aldrich, Steinheim, Germany

Saline solution (0.85%), University Hospital of North Norway, Tromsø, Norway

Trifluoroacetic acid for HPLC $\geq 99.0\%$, Merck, Darmstadt, Germany

Triton™ X-100, Sigma-Aldrich, St. Louis, Missouri, USA

Vancomycin hydrochloride from streptomycetes orientalis $\geq 80\%$, Sigma-Aldrich, St. Louis, Missouri, USA

6.2 Equipment

Atlantis T3 5 μm 4.6 x 20 mm guard cartridge, Waters, Milford, Massachusetts, USA

Dialysis membrane, MWCO 12-14000 Daltons, Medicell Membranes Ltd, London, UK

Cellophane foil, Bringmann folia, Wedelstein, Germany

Corning® UV-plate 96 well transparent, Corning Incorporated, Corning, New York, USA

Folded capillary zeta cell DTS1070, Malvern Panalytical, Malvern, UK

Nova-Pak® C18 60Å 4 μm 3.9 x 150mm HPCL-column, Waters, Milford, Massachusetts, USA

Nuclepore® Track-Etched Membranes polycarbonate, 0.8 μm , 0.4 μm , 0.2 μm , Whatman plc, Maidstone, UK.

Nunc™ EasyFlask™ 75cm² Nunclon™ Delta Surface, Thermo Fisher Scientific, Waltham, Massachusetts, USA

Spectra/Por® 4, Dialysis membrane tubing, MWCO:12-14 kD, Spectrum Laboratories Inc., Waltham, USA

Sterile Syringe Filter 0.2 µm, VWR International, Radnor, Pennsylvania, USA

6.3 Instruments

Accumet®, Portable pH-meter, AP115, Fisher Scientific, Waltham, Massachusetts, USA

Branson 5510, Branson Ultrasonic cleaner, Branson Ultrasonics Corporation, Danbury, Connecticut, USA

Büchi rotavapor R-124, Büchi Vacuum Pump V-700, Büchi Vacuum Controller V-850, Büchi Waterbath B-480, Büchi Labortechnik, Fawil, Switzerland

Cito-UNGUATOR® 2000, GAKO International GmbH, München, Germany

IKA® Vortex 3, IKA®-Werke GmbH & Co. KG, Staufen, Germany

Malvern Zetasizer Nano Zen 2600, Malvern Panalytical, Malvern, UK

McFarland DEN-1 densimeter, Biosan, Riga, Latvia

MGW LAUDA RM3 Thermo-Star water bath heater, Lauda-Brinkmann, Delran, New Jersey, USA

NICOMP Submicron particle sizer model 370, Particle sizing system, Santa Barbara, USA

Puranity PU 15+, Ultrapure Water System, VWR International, Radnor, Pennsylvania, USA

Rotavisc hi-vi II Complete viscometer, IKA®-Werke GmbH & Co KG, Staufen, Germany

Sension™+ PH31 pH-meter, HACH, Ames, Iowa, USA

TA.XT.plus Texture Analyser with backward extrusion rig, Stable Micro Systems Ltd., Surrey, UK.

Tecan Spark M10 multimode plate reader, Tecan Group Ltd., Männedorf, Switzerland

Waters 996, Photo array detector for HPLC, Waters Corporation, Milford, Massachusetts, USA

Waters 2690 HPLC separation module, Alliance HT, Waters Corporations, Milford, Massachusetts, USA

6.4 Software

Exponent Stable Micro Systems version 6.1.16.0, Texture Technologies Corporation, Hamilton, Massachusetts, USA

IKA Rotavisc Hi-Vi II, Labworldsoft 6.2.3.2, IKA-Werke GmbH & Co.KG, Straufen im Breisgau, Germany

ImageJ, version 1.53, National Institute of Health, Bethesda, Maryland, USA

Millennium³², version 3.20, Water Corporation, Milford, Massachusetts, USA

NICOMP CW388 Application version 1.68, Santa Barbara, USA

Tecan sparkcontrol method editor vesion 2.3, Tecan Group Ltd., Männedorf, Switzerland

Zetasizer Software, version 7.13, Malvern Panalytcs, Malvern, UK.

6.5 Biologicals

S. aureus MSSA476, BAA-1721™, ATCC, Manassas, Virginia, USA

E. coli 215922™, ATCC, Manassas, Virginia, USA

Murine macrophage RAW 264.7, ATCC, Manassas, Virginia, USA

7 Methods

7.1 Preparation of empty liposomes

Preparation of liposomes was based on the established thin film method (48). Lipoid S100 (200 mg) was weighed directly into a round bottom flask. Roughly 10 mL of methanol (MeOH) was added and hand-shaken until dissolved. The MeOH evaporated on Büchi rotavaporator at 60 mBar, 45°C and 60 rpm for at least 1 hour. The lipid film was rehydrated with 10 mL of distilled water and hand-shaken until the film had dislodged from the flask wall. Liposomal dispersion was stored overnight in cold storage conditions at 4-8°C prior to size reduction.

7.2 Preparation of drug-loaded liposomes

When preparing liposomes loaded with chosen SMAMP, from here on referred to as 8b, 10 mg of the was weighed directly into the round bottom flask together with 200 mg of Lipoid S100. Roughly 10 mL of MeOH was added and hand-shaken until dissolved, before evaporation under same conditions as empty liposomes. When incorporating CGA into the liposomes, the lipid film was rehydrated with a solution of 20 mg CGA in 10 mL of distilled water and hand-shaken until the film had dislodged from the flask wall. Liposomal dispersion was stored overnight in cold storage conditions at 4-8°C.

7.3 Size reduction of liposomes: Membrane extrusion

Size reduction of liposomes was executed by manual extrusion with Nuclepore® polycarbonate membranes. Filters with pore size 0.8 µm were utilized three times, 0.4 µm five times and 0.2 µm one time. Vesicle size was estimated with the Zetasizer to ensure correct number of extrusions and proper size. Extruded liposomes were stored in cold storage conditions overnight at 4-8°C before characterization.

7.4 Characterization of liposomes

7.4.1 Analysis of vesicle size and polydispersity index

The measurement of vesicle size and polydispersity index (PI) was carried out by photon correlation spectroscopy (PCS). To avoid contamination, the samples were prepared in a laminar flow cabinet. The liposomal dispersions were diluted in filtered (0.2 μm) distilled water until reaching an intensity of 250-350 kHz (49). The measurement was performed in three cycles, each with a run time of 15 minutes. These were done at room temperature $24 \pm 1^\circ\text{C}$ and with a scattering angle of 90 degrees. Results from the analysis are presented as the intensity weighted distribution.

7.4.2 Zeta potential

Determination of zeta potential was performed with the Zetasizer Nano Zen 2600. The liposomal suspension was diluted to 1 mL of an appropriate concentration with filtrated tap water (0.2 μm). The suspension was transferred to a clean zeta cell and zeta potential measured in three replicated at room temperature ($24 \pm 1^\circ\text{C}$).

7.4.3 pH

The pH of liposomes was measured using either Accumet® portable pH meter or Sension™+ PH31 pH-meter at room temperature ($24 \pm 1^\circ\text{C}$).

7.4.4 Entrapment efficiency

7.4.4.1 Separation: Dialysis

Separation of entrapped and freely distributed drug in liposomal dispersion was done through dialysis of 1:500 (v/v) in distilled water. First, the Spectra/Por® 4 dialysis membrane was conditioned in distilled water for 30 minutes. The dialysis membrane was then filled with liposomal dispersion and submerged in the container of water. The dialysis was conducted for 4 hours at slow stirring in room temperature ($24 \pm 1^\circ\text{C}$).

7.4.4.2 Entrapment efficiency - quantification of active substances

Quantification of entrapped CGA and 8b as done through HPLC.

Samples injected from each batch were non-separated liposomal dispersion (1:40) in MeOH, separated liposomal dispersion (1:40) in MeOH and water phase from dialysis. Three injections per sample were analyzed with an injection volume of 20 μ L.

Mobile phases utilized in the analysis were 0.1% (v/v) TFA in Milli-Q water (A) and 0.1% (v/v) TFA in acetonitrile (B). Phase distribution throughout the run can be shown in Table 1. A 5-minute delay was added in between each run.

Table 1: Programmed flow for mobile phase distribution in HPLC analysis

Time (min)	Flow (mL/min)	% A	% B
0.0	0.50	90.0	10.0
27.5	0.50	35.0	65.0
27.6	0.50	90.0	10.0

Detection was observed at wavelength 231 nm for 8b and 325 nm for CGA. To quantify the amount of active substance, a standard curve was constructed and used for calculation of concentration.

The entrapment efficiency (EE) was found by comparing the amount in dialyzed dispersion to the total amount of active substance in original sample. The entrapment efficiency was given as a percentage.

$$\frac{[\text{drug in dialyzed dispersion}]}{[\text{drug in original sample}]} \times 100\%$$

7.5 Hydrogel preparation

7.5.1 Plain chitosan hydrogel

Chitosan M (4.5% w/w) and 9% (w/w) glycerol in 2.5% (w/w) acetic acid in distilled water was weighed directly into the cito-unguator container. Subsequently the mixture was stirred with the Cito-UNGUATOR® before bath sonication for 30 minutes, followed by swelling for 48 hours at room temperature ($24 \pm 1^\circ\text{C}$) before characterization.

7.5.2 Liposomes in chitosan hydrogel

A hydrogel containing 5% (w/w) chitosan M and 10% (w/w) glycerol in 2.5% (w/w) acetic acid in distilled water was produced in the same way as in section 7.5.1 and left to swell for 48 hours at room temperature ($24 \pm 1^\circ\text{C}$) before incorporation of liposomes.

The liposomes were made, extruded and separated through dialysis as previously described. Liposomal dispersion was evenly distributed in the hydrogel through stirring by hand for 5 minutes. Adding 10% (w/w) of liposomal dispersion into the hydrogel resulted in a final concentration of 4.5% chitosan and 9% glycerol. The liposome-in-chitosan hydrogel formulation was stored in cold storage conditions overnight at $4-8^\circ\text{C}$ before characterization.

7.5.3 Chitosan hydrogel with free drug

For comparing purposes, a chitosan hydrogel with freely distributed drug (0.1 mg/mL 8b, 0.2 mg/mL CGA), 4.5% chitosan M and 9% glycerol was made. The active substances, 8b and CGA, were dissolved in glycerol and 2.5% (w/w) acetic acid in distilled water by magnetic stirring. Chitosan M was added before the mixture was stirred with Cito-UNGUATOR® and bath sonicated for 30 minutes, followed by swelling for 48 hours at room temperature ($24 \pm 1^\circ\text{C}$).

Table 2: Overview of studied hydrogel formulations and their components

Formulation	Components
HG	Chitosan Glycerol
HG-LIP	Chitosan Glycerol Empty liposomes
HG-LIP-CGA	Chitosan Glycerol CGA-liposomes
HG-LIP-8b	Chitosan Glycerol 8b-liposomes
HG-LIP-8b-CGA	Chitosan Glycerol 8b-CGA-liposomes
HG w/ free drug	Chitosan Glycerol 8b CGA

7.6 Hydrogel characterization

The hydrogels were characterized to study the application, compatibility with skin and user-friendliness of the formulations.

7.6.1 Viscosity

Both viscosity and shear stress were measured on the Rotavisc hi-vi Complete (two days after production start) with a shear rate from 4 to 23.63 s⁻¹, at both room temperature 25 °C and skin temperature (32 °C).

7.6.2 Texture analyser

Determination of the hydrogel texture properties was performed on the Texture Analyser TA.XT Plus with backward extrusion rig. The testing conditions were based on previously optimized method (50). The container from the rig set was filled with 65 g of hydrogel, secured with a weight to avoid displacement during testing and a 35 mm disc utilized as the contact point for the probe. The texture analyzer was set to measure the compression force by submerging 10 mm into to gel and withdraw back to starting point. The trigger force was set to 10 g and the speed pre-test, test and post-test were set to 10, 4 and 4 mm/s, respectively. Each hydrogel was measured 5 times with a 10 second interval between each run for reproducibility purposes.

7.7 pH

The pH of hydrogels was measured using Accumeter® portable pH meter at room temperature (24 ± 1°C).

7.8 Stability testing of liposomes and hydrogels

To test the stability of both the liposome and hydrogel formulation, characterization was done after finished production and repeated 2, 4 and 12 weeks after production start.

7.8.1 Stability of liposomes

The different parameters were determination as described in 5.4. Entrapment efficiency was determined only for drug loaded liposomes.

7.8.2 Stability of hydrogel

The different parameters were determination as described in 5.6. Viscosity was determined after finished production and not repeated the following weeks.

7.9 *In vitro* release study: Franz cell diffusion

In vitro drug release measurement was done through Franz cell diffusion to assess quality of nanocarrier and estimate *in vivo* performance with high reproducibility (46). The release study was performed on both the drug loaded liposomal suspensions and the semisolid drug loaded liposome-in-hydrogel formulation shown in Table 3. Prior to the release study, the liposomal suspension where dialyzed as previously described to remove untrapped drug. A cellophane foil membrane was mounted on the Franz diffusion cell to retain nanoparticles while allowing released drug to permeate to the acceptor compartment. An aliquot of 600 μ L of the studied formulations were added in the donor chamber. The 5 mL acceptor chamber was filled with 2% (w/w) β -cyclodextrin acceptor medium to ensure sink conditions.

The release study was done under stirring with circulating water at 32° C. An aliquot of 250 μ L extracted from acceptor at hour 1, 2, 3, 4, 5, 8 and 24 after start. The extracted volume was replaced with fresh 2% (w/w) β -cyclodextrin medium. The drug amount in the extracted sample was quantified by HPLC.

Table 3: Formulations included in *in vitro* drug release testing by Franz cell diffusion.

Liposomal suspensions	Liposome-in-hydrogel formulations
LIP-CGA	HG-LIP-CGA
LIP-8b	HG-LIP-8b
LIP-8b-CGA	HG-LIP-8b-CGA

7.10 Anti-oxidative activity

The anti-oxidative effect of CGA was determined by DPPH and ABTS•+ radical scavenging. Both methods were based on those previously reported by Jøraholmen *et al.* (9).

7.10.1 DPPH Radical Scavenging

For the DPPH radical scavenging, 0.3 mL of both DPPH (60 μ M) in 96% ethanol and CGA (5, 10 and 25 μ M as final concentration) in 96% ethanol were mixed well before left in the dark at room temperature ($24 \pm 1^\circ\text{C}$) for 30 minutes. The radical scavenging activity of CGA was measured spectrophotometrically on Spark plate reader at 519 nm. The absorbance was used as an expression of antioxidant activity, as the violet color of DPPH radicals decrease with the potential anti-oxidative effect of CGA. Antioxidant activity of CGA was compared to the activity of vitamin C and E in identical concentrations and conditions (9).

7.10.2 ABTS•+ Radical Scavenging Activity

A day in advance, an ABTS•+ radical solution was made by mixing 3 mL of ABTS solution (7.4 mM) and 3 mL potassium peroxodisulphate solution (2.6 mM), then left overnight in room temperature ($24 \pm 1^\circ\text{C}$) to let the ABTS•+ radicals form and stabilize. On the day of testing the ABTS•+ radical solution was diluted to 100 mL in ethanol. An aliquot of 0.3 mL of ethanolic ABTS•+ solution and 0.3 mL of CGA solutions (5, 10, 25 and 50 μ M as final concentration) was mixed and left in dark at room temperature ($24 \pm 1^\circ\text{C}$) for 30 minutes. The radical scavenging activity of CGA was measured on Spark plate reader at 731 nm. The ABTS•+ radicals have a green color that fade when neutralized in the reaction with antioxidants, and the absorbance can therefore be used as an expression of antioxidant activity. Antioxidant activity of CGA was compared to the activity of vitamin C and E in identical concentrations and conditions (9).

7.11 Evaluation of cell compatibility

The murine macrophages RAW 264.7 cell line was used for *in vitro* evaluation of the toxicity of liposomal suspensions and liposome-in-hydrogel formulations. Cells were cultured in

Nunclon T75 flasks (75 cm²) with RPMI 1640 medium with 10% fetal bovine serum (FBS) and 1% penicillin-streptomycin (complete RPMI medium) at 37°C in 5% CO₂.

On the first day, macrophages were prepared for plating by diluting the cell suspension to 1x10⁵ cells/mL in complete RPMI medium. The cells were plated by adding 90 µL of the cell suspension in each well of a 96-well plate and incubated for approximately 24 hours at 37°C in 5% CO₂.

On the second day, after incubation, the cell growth was evaluated under microscope. An aliquot of 10 µL of drug formulation diluted in non-complete RPMI medium was added to the wells. Three different dilutions were tested, resulting in a final lipid concentration of 1, 10 and 50 µg/mL on the plates. A positive control with 10 µL diluted Triton-X (1:4 in medium) and a negative control with 10 µL complete RPMI medium were also tested. Plates were then incubated for 24 hours ± 15 minutes at 37°C in 5% CO₂.

On the third day, 10 µL of solution from the CCK-8 kit was added to each well and incubate at 37°C in 5% CO₂ for 4 hours. Plates were then evaluated at the Tecan Spark UV–VIS plate reader at 450 nm with reference set to 650 nm.

7.12 Antimicrobial evaluation

The *in vitro* evaluation of antimicrobial activity of the studied formulations was performed through a modified disc diffusion method (51), where the formulations were placed directly on bacteria covered agar plates for observation of inhibition zones.

Both diluted and non-diluted formulations were utilized in this evaluation. The hydrogel was diluted in 1:4 distilled water to allow for pipetting of the formulation. To mimic the concentration of active substance, the liposomal was tested in a dilution of 1:40 in distilled water. Non-diluted liposomal dispersion was also tested. A full list of formulations tested can be found in Table 4. A solution of 400 µg/mL vancomycin hydrochloride or chloramphenicol was used as a positive control (52;53).

Table 4: Overview of formulations in antimicrobial testing and their respective drug concentrations.

Formulations		Final concentration drug
Liposomes	Empty	-
	CGA	CGA: 2 mg/mL
	8b	8b: 1 mg/mL
	8b-CGA	8b: 1 mg/mL CGA: 2 mg/mL
Liposomes 1:40	CGA	CGA: 50 µg/mL
	8b	8b: 25 µg/mL
	8b-CGA	8b: 25 µg/mL CGA: 50 µg/mL
Hydrogel 1:4	Empty	-
	LIP-CGA	CGA: 50 µg/mL
	LIP-8b	AMP: 25 µg/mL
	LIP-8b-CGA	8b: 25 µg/mL CGA: 50 µg/mL
	8b-CGA (free)	8b: 25 µg/mL CGA: 50 µg/mL
Control <i>S. aureus</i>	Vancomycin hydrochloride	400 µg/mL
Control <i>E. coli</i>	Chloramphenicol	400 µg/mL

The testing was carried out on both a gram-positive and gram-negative bacterium, more specifically *S. aureus* MSSA476 and *E. coli* ATCC25922.

Firstly, a 0.5 McFarland of suspension of bacteria ($\sim 1 \times 10^8$ CFU/mL) in 0.85% NaCl solution was prepared. The bacterial solution was plated uniformly on a Mueller Hinton agar plate. Drops of 10 μ L of the drug formulation was then placed on the prepared agar plates. After drying, the plates were incubated for 24 hours at 37°C. After 24 hours, the plates were evaluated, and inhibition zones recorded. Zones were measured with the software ImageJ (54). The antibacterial activity was calculated as a percentage of the inhibition compared to the positive controls.

7.13 Statistical analyzes

Student's t-test was performed to determine statistical significance. A p -value ≤ 0.05 was considered statistically significant.

8 Results and discussion

8.1 Liposome vesicle characteristics and stability

8.1.1 Size

Size is a critical property in skin delivery, determining the penetration and fate of the drug carriers. The vesicles should be small enough to penetrate to desired tissue, but large enough to ensure necessary drug encapsulation and avoid systemic absorption (7;8). The aim was to produce liposomal vesicles suited for dermal application, with diameters of approximately 300 nm and $PI < 0.3$.

Measurements of size and size distribution over a 12-week period are presented in Table 5. Results from the PCS readings are expressed as mean particle size following Gaussian distribution and size distribution as PI.

The size measurements by PCS can be presented through two different distribution models; Gaussian or NICOMP. The Gaussian model can be applied to measurements following normal distribution, while the NICOMP is used for measurements of multimodal samples. Specific requirements for each model are described by Hupfeld *et al.* (49). Results in Table 5 are expressed following the Gaussian distribution, as the prevalence of this distribution was much greater than the NICOMP model for this data set.

Table 5: Size and size distribution for liposomal drug formulations over a period of 12 weeks. Each formulation was tested in 3 separate batches, with 3 measurements per batch. All values are expressed as mean \pm SD ($n=3$). Diameter measurement is intensity weighted. Week 0 = two days after production, one day after extrusion.

Formulation	Week	Mean diameter (nm)	PI
LIP	0	259.8 \pm 14.3	0.220 \pm 0.129
	2	257.5 \pm 12.4	0.174 \pm 0.077
	4	257.9 \pm 9.0	0.171 \pm 0.084
	12	261.2 \pm 9.1	0.160 \pm 0.032
LIP-CGA	0	223.7 \pm 5.6	0.235 \pm 0.059
	2	217.1 \pm 3.1	0.156 \pm 0.056
	4	218.0 \pm 3.5	0.152 \pm 0.051
	12	223.1 \pm 8.8	0.191 \pm 0.067
LIP-8b	0	216.1 \pm 16.0	0.128 \pm 0.040
	2	217.1 \pm 18.3	0.137 \pm 0.042
	4	213.7 \pm 15.4	0.133 \pm 0.042
	12	212.6 \pm 15.9	0.127 \pm 0.041
LIP-8b-CGA	0	208.4 \pm 2.5	0.083 \pm 0.017
	2	207.9 \pm 2.0	0.089 \pm 0.010
	4	202.6 \pm 0.6	0.084 \pm 0.008
	12	201.2 \pm 2.3	0.093 \pm 0.010

Liposomal suspension produced by the available preparation methods, such as the thin-film method, typically contain a heterogenous collection of multilamellar vesicle (MLV) with diameters over 1 μ m. The extrusion method is an easy way of controlling liposome size and

distribution, especially in the desired size range of this project. Extrusion outcome is dependent not only the polycarbonate filters used, but also the applied pressure. Average vesicle size decreases with increased pressure, which makes the extruded size dependent on the applied pressure from the individual carrying out the procedure (39).

Results in Table 5 shows mean diameters in the range of 200-300 nm, which is acceptable, and PI fitting for a dermal drug delivery system. The size also indicates the possibility of biofilm penetration, an important attribute in treatment of chronic wounds infected by biofilm producing bacteria. The size stability and homogeneity over time does not indicate any major aggregation in the suspension. Yet, this is just an assumption that can be confirmed through other methods, such as TEM imaging.

8.1.2 Zeta potential

Zeta potential plays a role in stability of the liposomal bilayer and is therefore important to monitor over time. Measurements for the four different liposomal suspensions over a 12 week-period are presented in Table 6.

Over the testing period, the ZP of empty liposomes were, as expected, in the neutral area between -10 mV and 10 mV. This is due to the phospholipid used in the making of our liposomes, phosphatidylcholine (PC). PC is a zwitterionic lipid with a positive choline group and a negative phosphate group, resulting in liposomes with neutral zeta potential (9;23).

Both liposomes containing 8b and dual-loaded liposomes incorporating 8b and CGA shows a strong positive charge. This is an expected result of the inclusion of 8b, which mimics the positive net charge of AMPs. With a ZP over 30 mV, we can expect the systems incorporating 8b to exhibit good physical stability. Cationic liposomes also have an increased ability to interact selectively with bacterial cells, possibly improving both efficacy and safety of the drug delivery system (10;31).

Table 6: Zeta potential of liposomal suspensions. Results are presented as mean with associated SD, n=3.

	Production +2 days		2 weeks		4 weeks		12 weeks	
	Mean [mV]	SD	Mean [mV]	SD	Mean [mV]	SD	Mean [mV]	SD
LIP	-2.9	2.4	-2.1	0.8	-4.7	1.4	-6.7	0.6
LIP-CGA	-6.8	7.5	-11.0	5.2	-12.6	3.0	-18.5	3.2
LIP-8b	46.0	1.0	43.1	1.4	47.4	3.0	45.0	1.6
LIP-8b- CGA	40.0	1.3	38.9	0.4	42.1	0.9	38.9	1.0

8.1.3 pH

pH measurement of liposomal suspensions was carried out largely to ensure stability over time. The pH of the four different liposomal suspensions was measured over the testing period of 12 weeks (Figure 11).

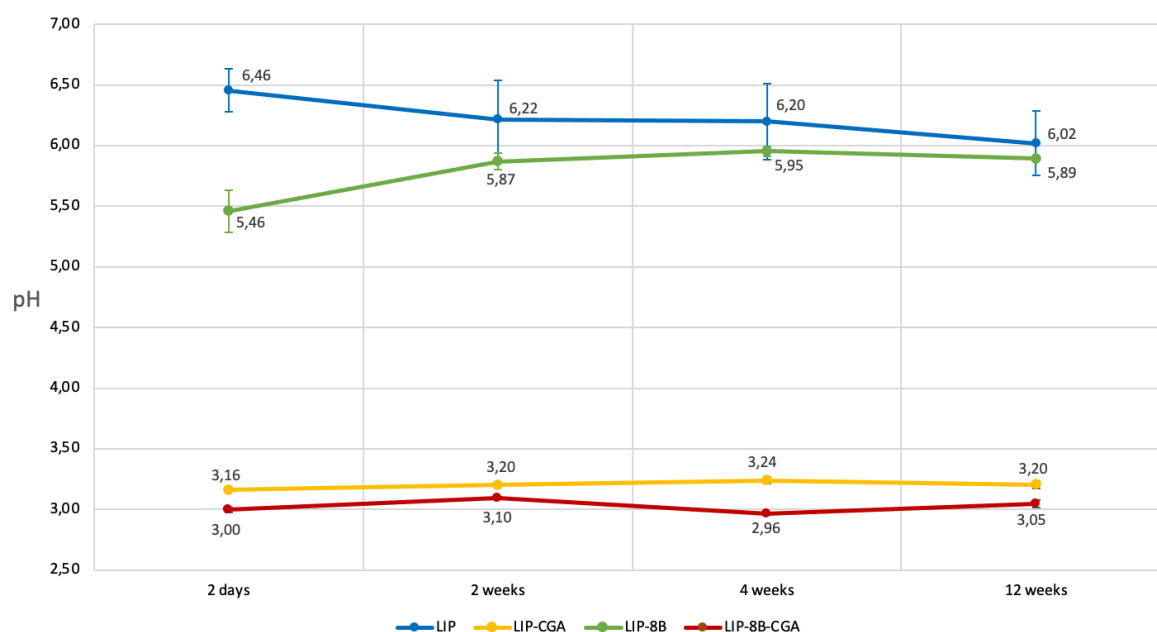


Figure 11: pH of all tested liposomal suspensions followed up for 12 weeks after production. Results are presented as mean \pm SD, n=3.

Of the four liposomal suspensions tested, the two containing CGA was found to have considerably lower pH when compared to the rest. This was expected as CGA is a carboxylic acid, resulting in a decrease in pH of the liposomal suspensions. Since liposomal suspensions are dependent on a second vehicle for topical application, the pH of liposome-in-hydrogel formulations should be considered as more important than liposomal suspension in terms of effect on wound healing.

8.1.4 Liposomal entrapment of active compounds

Characterization of EE is important to ensure predicable and adequate amount of active compound in the drug carrier, so that the novel drug formulation can provide effective treatment on administration site. This is especially important in antibacterial treatment, where sufficient drug concentration is required to eradicate bacteria. The EE of tested liposomal suspensions are presented in Figure 12, showing entrapment efficiency of both single- and dual-loaded formulations. Quantification of active compounds was performed by HPLC, and EE was calculated by comparing the amount in dialyzed dispersion to the total amount of active substance in original sample.

As previously discussed, liposomes can incorporate both lipophilic and hydrophilic drugs. The CGA is a hydrophilic compound added in preparation method together with the hydration media and should therefore be entrapped in the hydrophilic core of the liposomes. With the amphiphilic nature of SMAMP 8b and the fact that it was added in the organic solvent during the thin film preparation method, we expect it to be incorporated in the lipid bilayer. Its amphiphilic structure also enables distribution closer to the inner core and outer surface of the bilayer, possibly resulting in a relatively high entrapment (23).

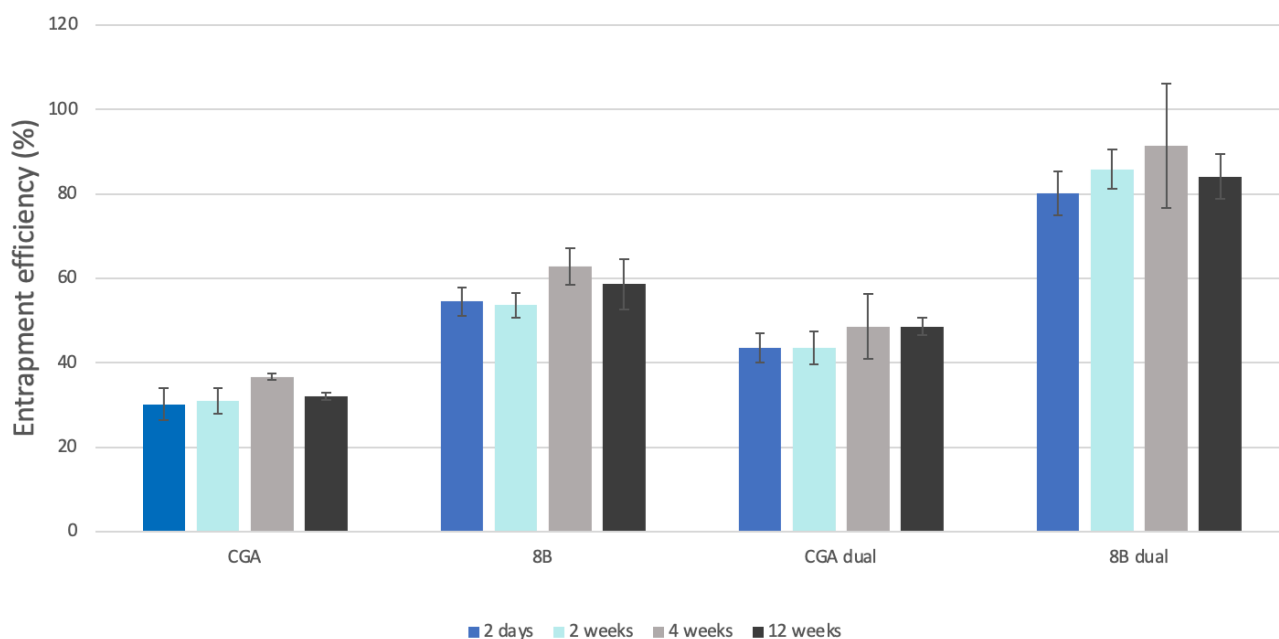


Figure 12: Entrapment of active compounds in liposomes, both as single- and dual-loaded formulations. Entrapment efficiency is given as a percentage of the amount of drug entrapped in liposomes compared to the total amount drug in the respective samples. Results are expressed as mean \pm SD, $n=3$.

The quantification of entrapped compounds show that dual-loaded liposomes have a greater EE than liposomes containing a single compound. This difference is visible for both CGA and 8b. At 12 weeks after production, 8b had an EE of $84.1 \pm 5.3\%$ and CGA $48.6 \pm 2.0\%$. With dual loading causing an increase in EE, it renders our drug delivery system more likely to deliver sufficient doses of active compound to the site of administration.

8.2 Hydrogel characteristics

8.2.1 pH of hydrogel

Intact human skin normally has a pH between 4 and 6. With a large number of pathogenic bacteria experiencing ideal growth conditions in neutral pH, and a more acidic environment is suggested to improve wound healing (10). When testing these novel dermal drug delivery

systems, it was important to control pH over time. The pH measurements over the 12-week stability testing are presented in Figure 13.

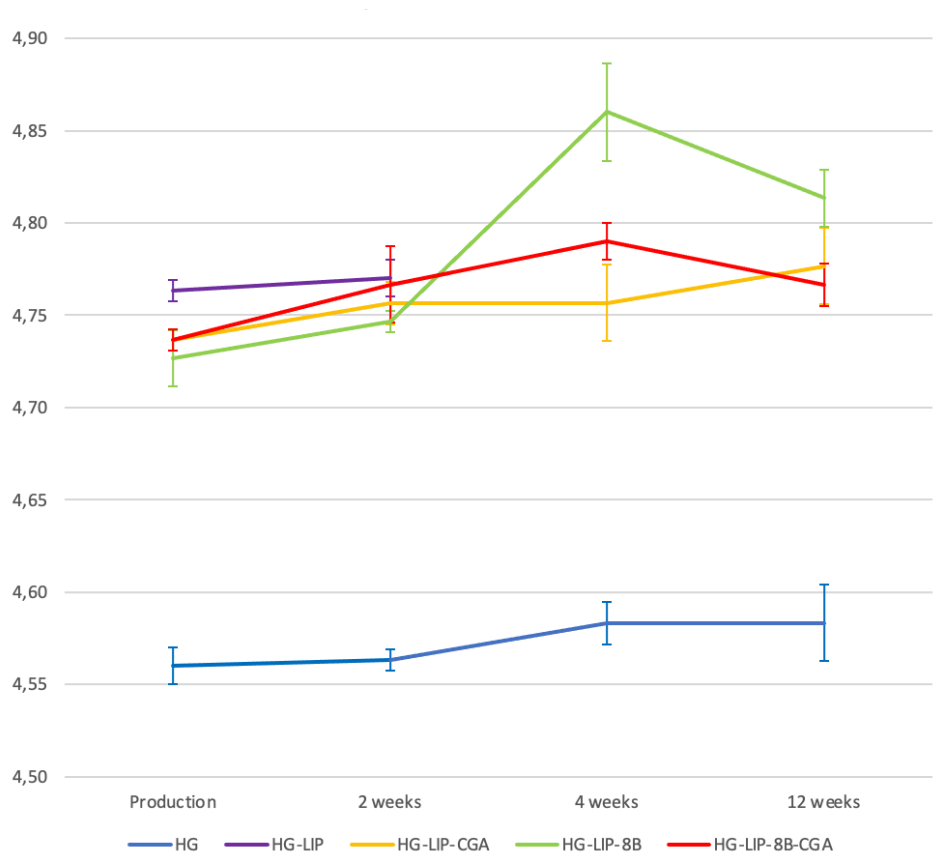


Figure 13: pH of liposome-in-chitosan-hydrogel formulations over the stability testing period of 12 weeks. Results are presented as mean \pm SD, $n=3$.

The empty chitosan hydrogel formulation stood out with a considerably lower pH compared to liposome-in-chitosan-hydrogel formulations. This is the result of the liposome-in-hydrogel formulations containing 10% (w/w) of liposomal suspension, while the plain hydrogel does not, and essentially substitutes the last 10% with 2.5% (w/w) acetic acid, decreasing the pH.

Stability of pH was considered relatively good, with the largest fluctuation seen in hydrogel containing liposomes loaded with 8b, with a mean of 4.73 ± 0.02 in the production week and 4.86 ± 0.03 in week 4.

All of the tested hydrogels had pH in the range of normal human skin under the entirety of the testing period. All tested hydrogels had a slightly acidic pH and could possibly support the healing ability of incorporated active compounds.

8.2.2 Viscosity

The aim of this project was to develop a delivery system able to prolong contact between drug delivery system and skin for an optimal therapeutic outcome. For this, optimal viscosity was required to assure good applicability, spreadability and bioadhesion, resulting in high user-friendliness (11).

The results from rheological testing of liposome-in-chitosan-hydrogel formulation of both unloaded and drug loaded liposomes are shown in Figure 14 and 15. Since rheological behavior is influenced by temperature (10), measurements were performed at both room temperature (25°C) and skin temperature (32°C).

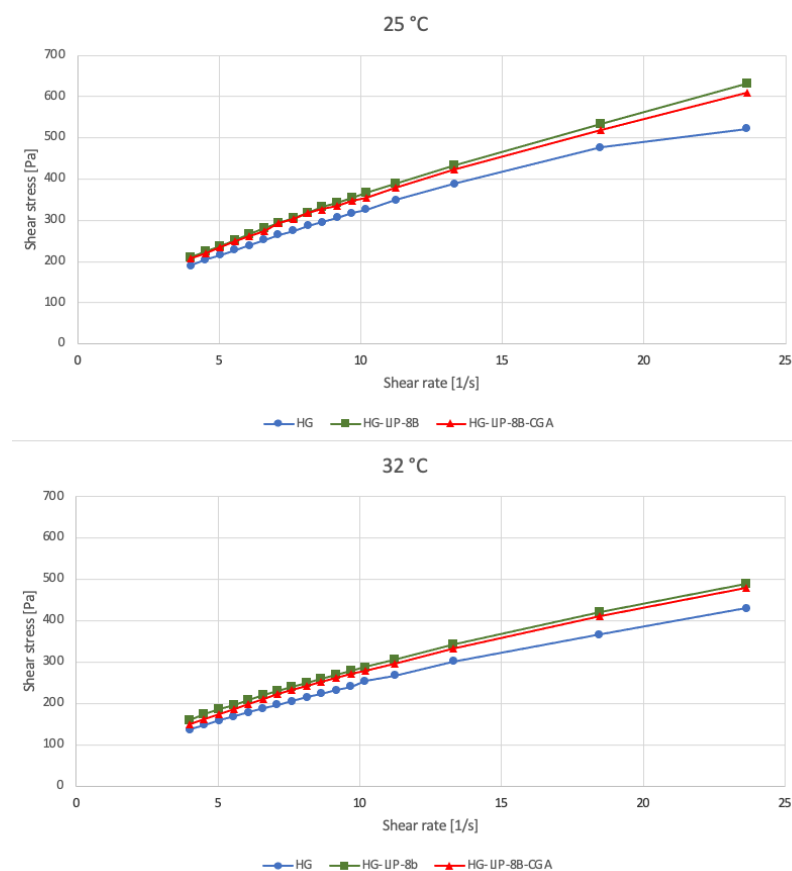


Figure 14: Shear rate plotted against shear stress for three different hydrogel formulations at 25 °C and 32 °C.

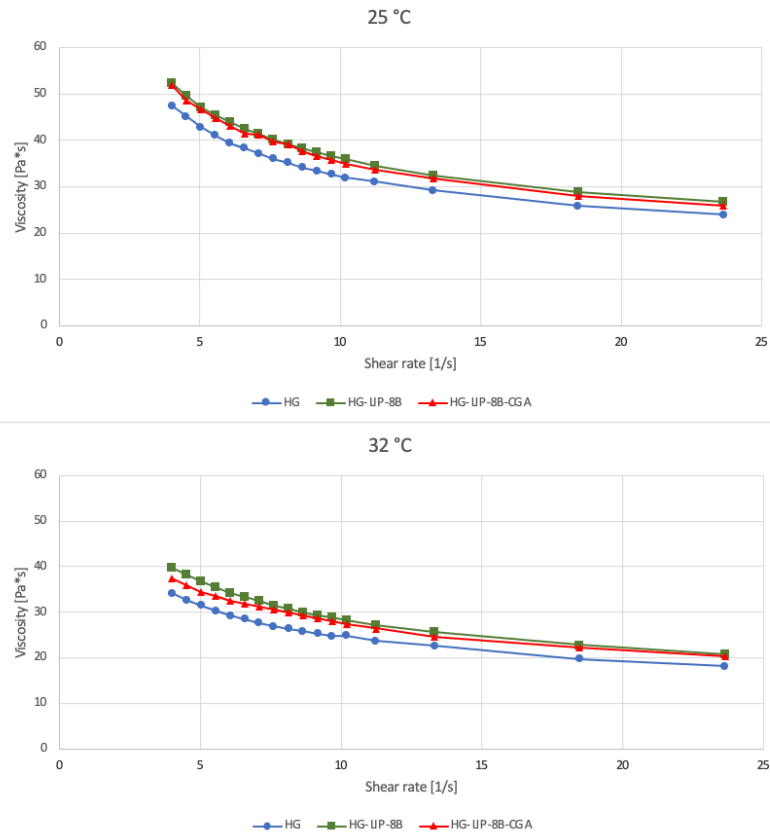


Figure 15: Viscosity plotted against shear stress for three different hydrogel formulations at 25 °C and 32 °C.

As previously described, the chitosan polymer is a viscosity enhancing agent. Chitosan hydrogels show pseudoplasticity with a characteristic decrease in viscosity with increased shear rate. An increase in temperature should decrease viscosity (14). This pseudoplastic behavior was demonstrated for all three formulations. Viscosity was also lowered at 32°C compared to 25°C. The pseudoplastic behavior is considered suitable for topical formulations as it ensures uniform distribution on skin (55).

Liposomes are made from phospholipids, also known to act as plasticizers, able to increase the mobility of the polymer network in hydrogels. This effect could not be observed in obtained results, corresponding with the findings of Hemmingsen *et al.* (10). The incorporation of liposomes instead affected the rheology of chitosan hydrogel by causing a small increase to viscosity.

8.2.3 Texture properties

The mechanical properties of hydrogels are important for effectiveness and applicability. The aim of conducting texture analysis and measure the texture properties hardness, cohesiveness and adhesiveness, was to determine the effect of incorporated liposomes, as well as monitoring the hydrogel stability over time. Based on previous work, expectations were that the incorporation of liposomes in the hydrogel could affect the texture properties (9;10). The measurements at 2 and 12 weeks after production are presented in Figure 16 and 17. Complete overview of the stability of all 4 formulations at production, week 2, week 4 and week 12 can be found in Appendix I.

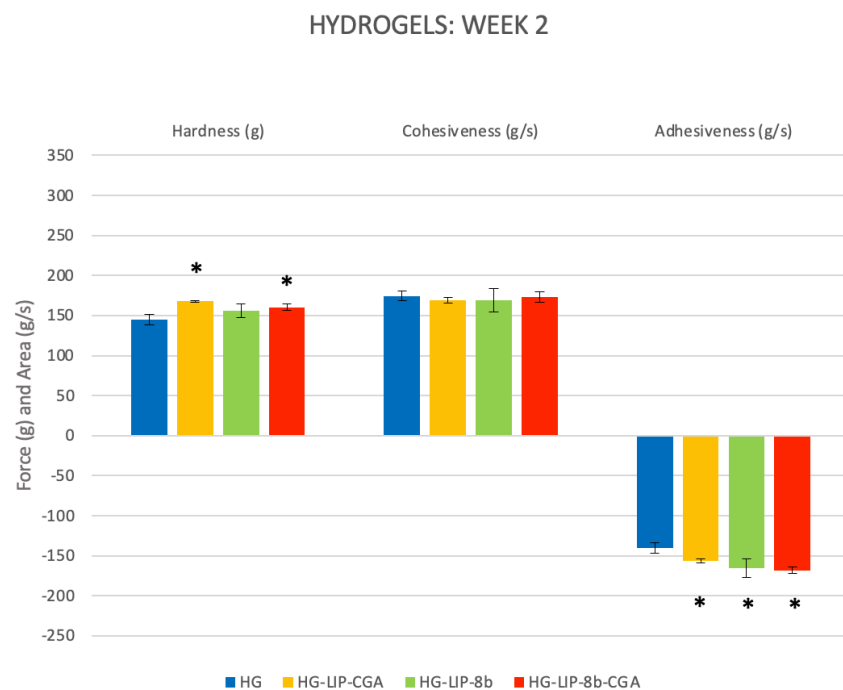


Figure 16: Comparison of texture properties at 2 weeks after production. Results are presented as mean \pm SD, $n=3$. * $p<0.05$ compared to empty chitosan hydrogel.

At week 2, all hydrogel formulations had relatively similar texture properties. Formulations incorporating CGA had a statistically significant increased hardness compared to empty hydrogel. An increase in hardness could also be seen for liposome-in-hydrogel formulation incorporating 8b, although not statistically significant. A greater adhesiveness was observed for all formulations with liposomes, and the difference to empty hydrogel was statistically significant. These findings are supported by Jørholm *et al.* (9), although they observed an

increase in all parameters for hydrogels containing liposomes. This was not observed for the cohesiveness of our formulations.

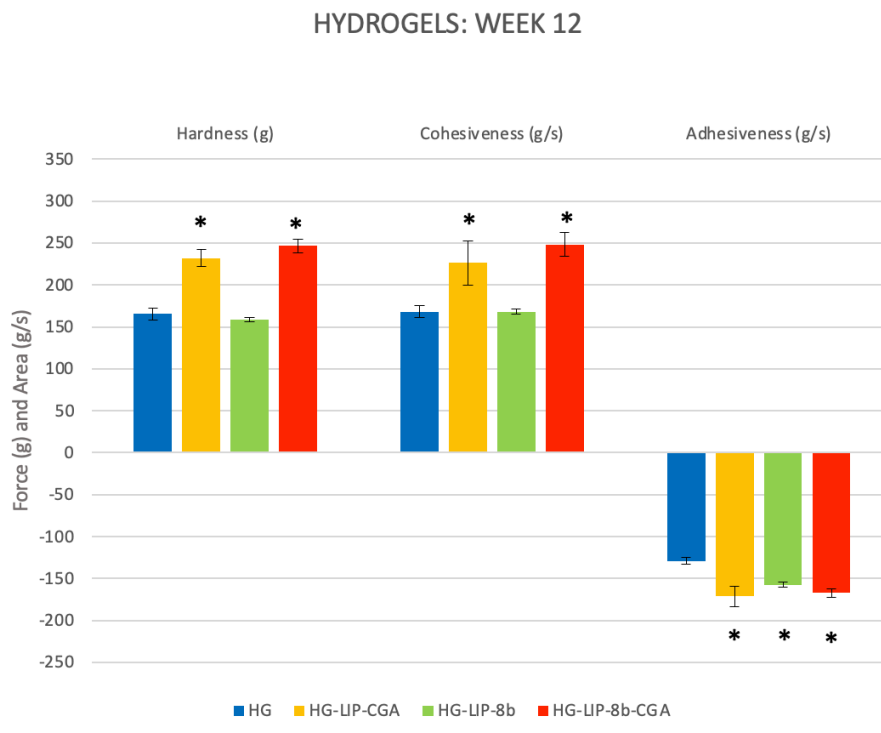


Figure 17: Comparison of texture properties at 12 weeks after production. Results are presented as mean \pm SD, $n=3$. * $p<0.05$ compared to empty chitosan hydrogel.

All formulations were relatively stable over the first 4 weeks. At week 12, a large increase in hardness and cohesiveness could be observed for liposome-in-hydrogel formulations containing CGA. This increase occurred in the period between week 4 and 12, see Appendix I. The change in properties could not be seen for adhesiveness, nor any of the texture properties of plain hydrogel or liposome-in-hydrogel incorporating 8b. These two formulations were relatively stable over the 12-week period. The instability caused by the introduction of CGA could be an issue, as tailoring the texture properties could be more challenging when they change significantly over time.

8.3 *In vitro* release study: Franz cell diffusion

The determination of drug release from a formulation is one of the most important estimates of *in vivo* performance, as it reveals information on drug penetration through skin and release kinetics, used to assess both effect and safety. The release of active compounds from both liposomal suspensions and liposome-in-hydrogel formulations was determined by Franz cell diffusion and quantification by HPLC. The Franz diffusion cell has the advantage having both high reproducibility and being a good method for testing both colloidal and semi-solid formulations (46).

Tested formulations are listed in Table 3. The chosen acceptor medium was 2%(w/w) β -cyclodextrin. Results from the drug release testing can be seen in Figure 18.

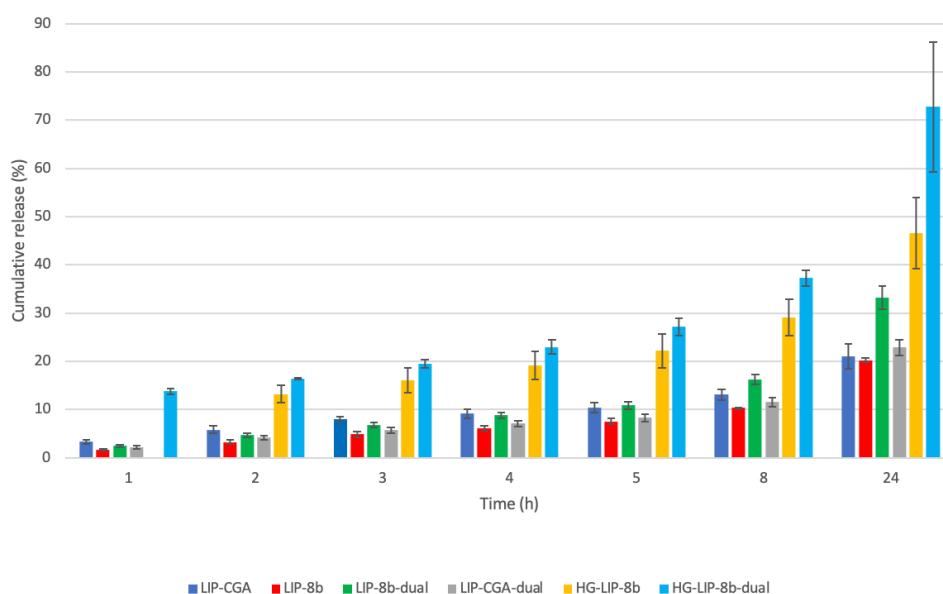


Figure 18: Drug release from liposomal suspensions and liposome-in-hydrogel formulations over 24 hours at 32 °C. The release is presented as a percentage of the total amount of entrapped drug, calculated from the amount established through entrapped testing. Results are expressed as mean \pm SD, n=3.

In general, a greater release could be seen from liposomes-in-hydrogel compared to liposomal suspensions. This result was unexpected, as the findings of Hemmingsen *et al.* (10) showed that incorporation of liposomes in hydrogel resulted in lower release of a membrane-active antimicrobial compared to liposomal suspension. An effective release of SMAMP from both single- and dual-loaded liposomes-in-hydrogel formulations is a positive result, however, this must be further tested to assure reproducibility.

CGA incorporated in liposome-in-hydrogel formulations, both single- and dual loaded, are not included in Figure 18. Release of CGA from these formulations was not sufficient to calculate release over time. In contrast, release of the same compound from liposomal suspension showed stable release, with a release of $21.0 \pm 2.6\%$ for single-loaded formulation and $22.9 \pm 1.7\%$ for dual-loaded. As the addition of hydrogel limited the drug release, it may be possible that CGA has a higher affinity for the hydrogel than acceptor medium, but as this is not clear and further testing is required.

Drug release testing was performed over a period of 24 hours, with more frequent testing the first 8 hours. This was to determine both initial and more long-term release. A desired property for a dermal drug formulation for chronic wounds is sustained release over a longer period to assure a constant antibacterial, as well as an acceptable frequency of application. Presented in Figure 19 is the release over time of 8b from our final formulation, dual-loaded liposome-in-hydrogel formulation. This shows a sustained release over 24 hours, indicating the possibility of effective treatment, while only requiring change of wound dressing once daily. These attributes could increase user-friendliness and cause less physical strain from application.

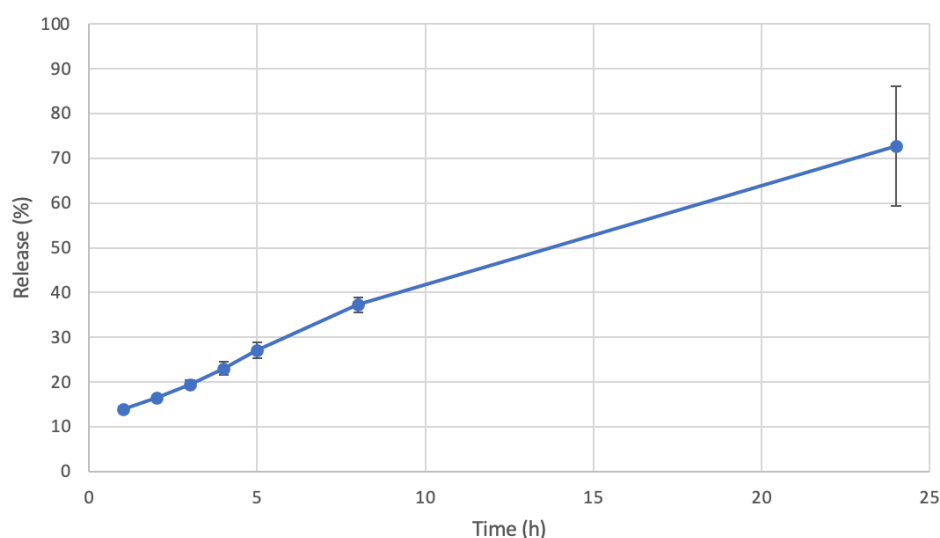


Figure 19: Release of 8b from liposome-in-hydrogel formulation loaded with both CGA and 8b over a 24-hour period. The release is presented as a percentage of the total amount of entrapped drug, calculated from the amount established amount through entrapped testing. Results are expressed as mean \pm SD, $n=3$.

One thing to keep in mind, is that hydrogels have the ability to absorb fluid (12). During the release study, hydrogels visibly swelled over time as it absorbed water from the acceptor compartment. This could have affected release and calculation of released amount during

testing. This could also be a challenge *in vivo* when applied to wounds with substantial amounts of wound exudate.

Another factor that could have affected the results, is that liposomal suspensions were not diluted prior to testing. The consequence of this is that suspensions were tested on Franz cells with a 10-times higher concentration of lipids and active compounds compared to liposome-in-hydrogel formulations, The difference in concentration was adjusted for during calculations, but the different testing conditions could not be adjusted for, possibly affecting the results.

8.4 Anti-oxidative activity

Since over-production of ROS may delay wound healing, determining the anti-oxidative effect of CGA was important to assess potential wound healing properties (32). The radical scavenging activity of CGA was compared to well-known antioxidants vitamin C and E (9). The result of anti-oxidative assay through ABTS and DPPH radical scavenging activity is presented in Figure 20 and 21, respectively.

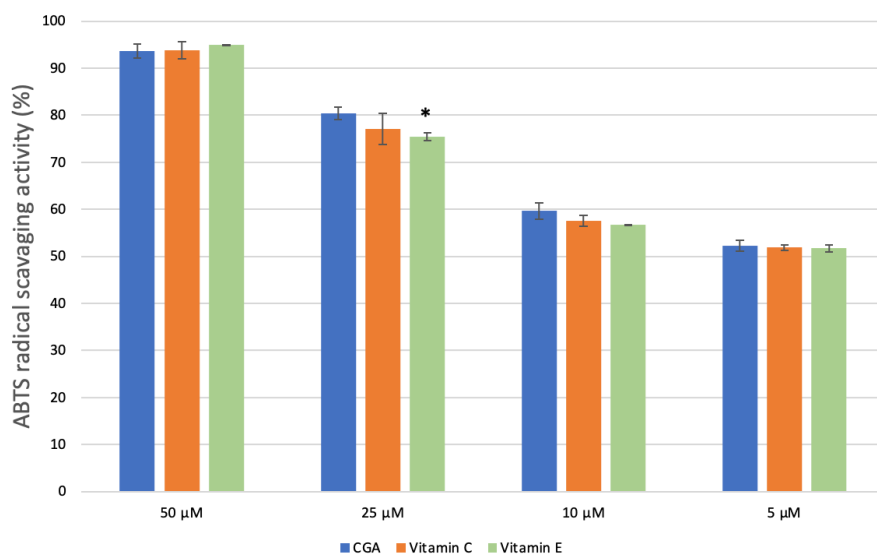


Figure 20: Anti-oxidative activity of CGA compared to vitamin C and E in ABTS radical scavenging. All antioxidants were tested at concentration 50 μM, 25 μM, 10 μM and 5 μM. Results are expressed as mean ± SD, n=2. * p<0.05 compared to CGA in corresponding concentration.

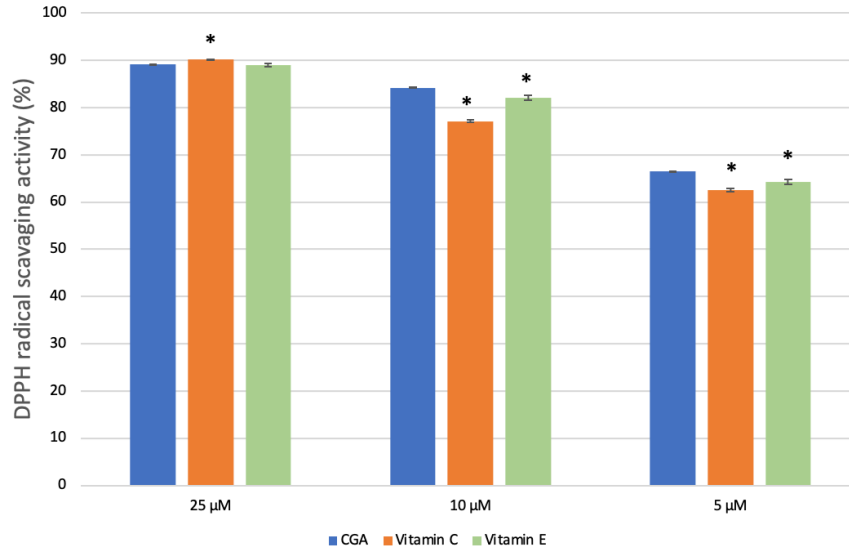


Figure 21: Anti-oxidative activity of CGA compared to vitamin C and E in DPPH radical scavenging. All antioxidants were tested at concentration 25 μM , 10 μM and 5 μM . Results are expressed as mean \pm SD, $n=2$. * $p<0.05$ compared to CGA in corresponding concentration.

Testing results show that the antioxidative effect of CGA is comparable to both vitamin C and E. The ABTS radical scavenging showed no statistically significant difference in antioxidative effect, except for comparison of CGA and vitamin E at the concentration of 25 μM , where CGA showed a higher mean percentage of radical scavenging. Results from the testing of higher concentrations of antioxidants show that the radical scavenging seemed to plateau at approximately 90%. This was the case for ABTS radical scavenging with 75 μM samples, and DPPH radical scavenging with 50 μM and 75 μM samples. These results were therefore not included in figures.

In the DPPH radical scavenging CGA showed a statistically significant difference in antioxidative effect compared to both vitamin C and E at lower concentrations, 10 μM and 5 μM . For these concentrations, the radical scavenging of CGA was higher than both vitamin C and E.

In this project, we aimed for a multi-targeted approach with our dual-loaded liposome-chitosan-hydrogel system. The results demonstrating the adequate anti-oxidative effect of CGA suggests that our formulation could help limit ROS, often overproduced in chronic wounds, and therefore potentially improve wound healing (32).

8.5 Cell compatibility

The cell toxicity study was carried out on the murine macrophage RAW 264.7 cell line to assess cell compatibility. Investigating possible toxic effects in macrophages is important as they have a central role both in both pro-inflammatory and anti-inflammatory processes. In the inflammatory phase, typically after an acute wound, pro-inflammatory M1 macrophages remove pathogens and debris to accelerate wound healing and avoid infections. The M2 phenotype has anti-inflammatory abilities and is most present in the proliferation phase (56). With this new drug delivery system, it was important to ensure that the formulation did not induce toxicity and cell death to macrophages, risking further damage to the wound.

Cell compatibility of liposomal suspensions are shown in Figure 22, and for liposome-in-hydrogel formulation in Figure 23.

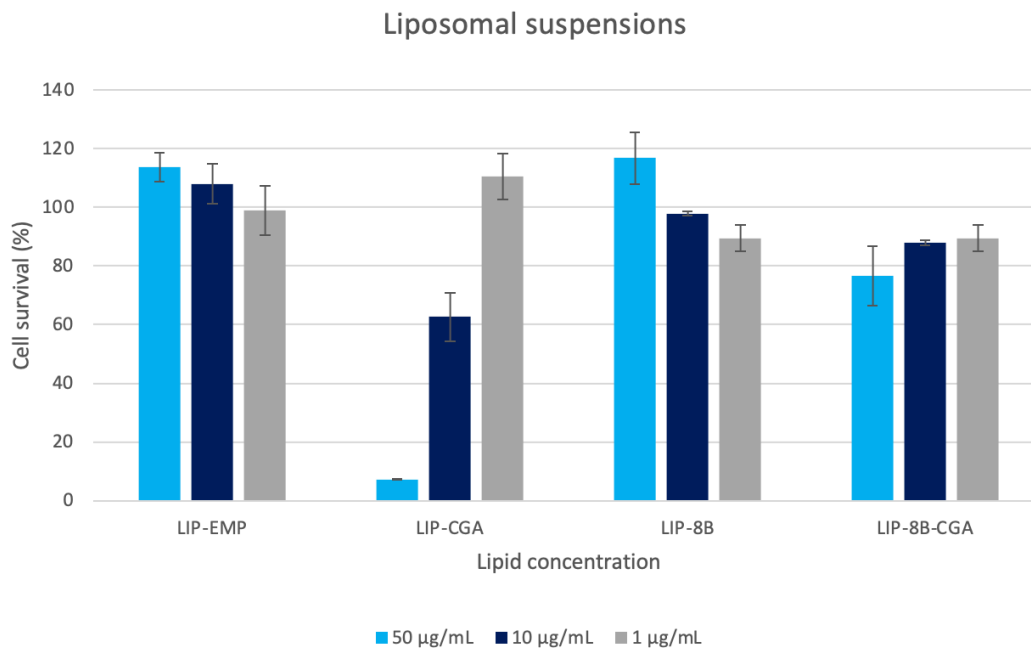


Figure 22: Results of cell toxicity testing of liposomal suspensions on macrophages. Diluted formulations were added on the plates, resulting in an end lipid concentration of 50 µg/mL, 10 µg/mL and 1 µg/mL in the wells. Results are expressed as the percentage of cell survival in treated cells compared to untreated cells. Results are presented as mean \pm SD, n=3.

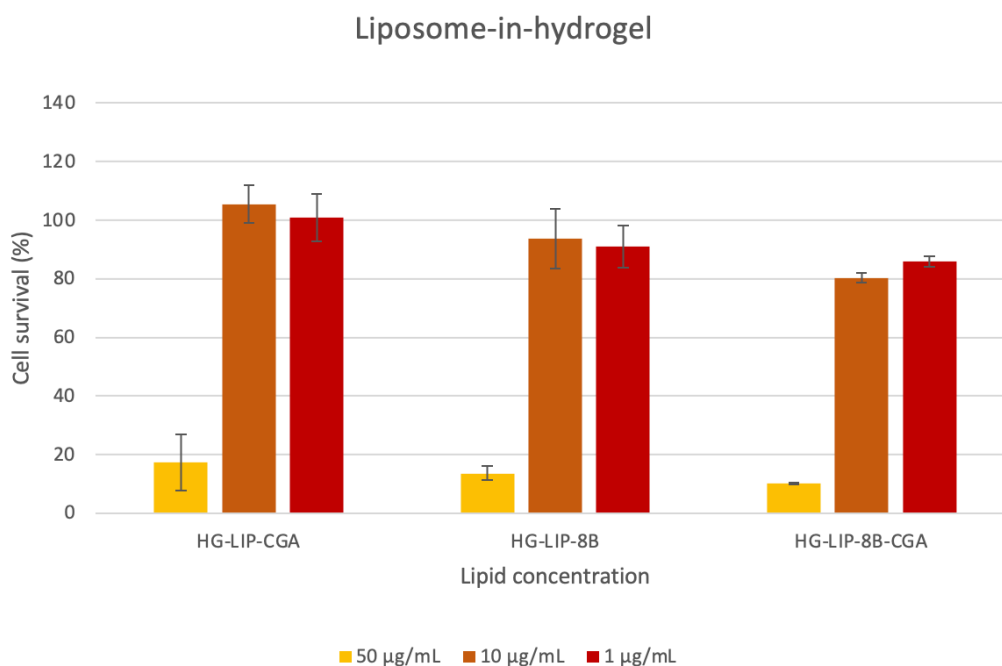


Figure 23: Results of cell toxicity testing of liposome-in-hydrogel formulations on macrophages. Diluted formulations were added on the plates, resulting in an end lipid concentration of 50 µg/mL, 10 µg/mL and 1 µg/mL in the wells. Results are expressed as the percentage of cell survival in treated cells compared to untreated cells. Results are presented as mean ± SD, n=3.

Results show that selected formulations have cytotoxic effects on macrophages. By the ISO standard of determination of *in vitro* cytotoxicity, a reduction of cell viability by more than 30% is considered cytotoxic (57). The liposomal suspensions containing CGA with a lipid concentration of 50 µg/mL and 10 µg/mL, exceeded this threshold, showing a mean cell survival of $7.3 \pm 0.1\%$ and $62.6 \pm 8.1\%$, respectively. All hydrogels with lipid concentrations of 50 µg/mL also fell into this category.

These findings were unexpected since, as previously mentioned, both CGA and chitosan-hydrogels are considered to have minimal to no toxic effects. Chitosan has previously been found to have no cytotoxic effect in murine macrophages (58). Hemmingsen *et al.* carried out an evaluation of toxicity of chitosan hydrogel incorporating a membrane active antimicrobial, showing no toxicity in keratinocytes of identical empty chitosan hydrogel (10).

These results suggest that further toxicity testing should be performed on these formulations, in both macrophages and other relevant cell lines, such as keratinocytes and fibroblasts. The potential for toxic effects of CGA should be explored further through testing of free compound.

This could be done by testing of a range of different concentrations on macrophages and other cell types.

8.6 Antimicrobial testing

Bacterial infections are a burden to wounds, slowing down or completely hindering wound healing (12;18;19). All of the incorporated active compounds in our formulation, the SMAMP 8b, CGA and the chitosan polymer have demonstrated antibacterial effects (1;34). To assess the possibility of synergetic antimicrobial effect, both liposomal suspensions and liposome-in-hydrogel formulations were tested through a modified disk diffusion method.

Both liposomal suspensions and liposome-in-hydrogel formulations were included in antimicrobial testing on gram-positive and gram-negative bacteria to assess their potential bacterial inhibition when applied to infected wounds. The two bacterial species, *S. aureus* and *E. coli*, are frequently found in infections of chronic wounds (1). Hydrogels were diluted 1:4 to achieve viscosity suitable for pipetting onto agar plates. To correspond with concentration of lipids and active compounds of diluted hydrogel, liposomal suspensions were diluted 1:40. Specific tested formulations are listed in Table 4. As positive controls, vancomycin was added on plates with gram positive *S. aureus*, while chloramphenicol as utilized as control for gram negative *E. coli*. The antibacterial activity of tested formulations was expressed as a percentage of the diameter of inhibition zone compared to controls, considered as 100%. Final results are displayed in Figure 24.

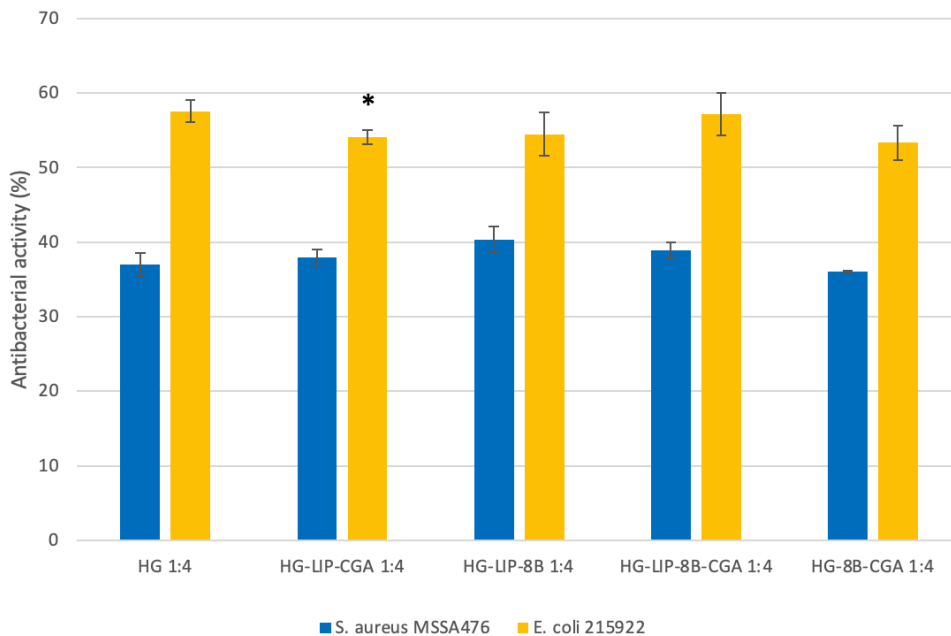


Figure 24: Antibacterial activity of liposome-in-chitosan-hydrogel formulations compared to a chitosan hydrogel with free active compounds. The antibacterial activity is expressed as the percentage of inhibition area for respective formulations compared to positive controls (100%). Results are expressed as mean \pm SD, $n=3$. * $p<0.05$ compared to empty chitosan hydrogel (HG 1:4).

All hydrogel formulations demonstrated antibacterial activity in both *S. aureus* and *E. coli*. There were no statistically significant differences in activity of drug loaded hydrogels and empty chitosan hydrogels, except for CGA-loaded liposome-in-hydrogel formulation, having a smaller diameter of inhibition zone when plated *E. coli*.

Liposomal suspension showed no antibacterial activity in neither *S. aureus* nor *E. coli*. One exception was undiluted liposomal suspension of CGA and 8b, showing partly inhibition of *S. aureus* in the area of application. Picture can be found in Appendix II. The lack of antibacterial activity is most likely due to the testing method, where the liposomal suspensions dried out on the agar plates, possibly harming the integrity of liposomes and change their ability of drug delivery.

The method of testing may also be unsuited for characterizing the effects of the active compounds in the liposome-in-hydrogel formulations. The similar inhibition areas of the tested formulations could indicate that the antibacterial inhibition only demonstrates the effect of chitosan. A possible explanation could be the drying of the hydrogel and liposomes on the agar plate, decreasing the ability of drug delivery. This makes characterizing the effects of the two

active compounds in the liposome-in-hydrogel formulations difficult. Further testing should be performed to investigate the effects of active compounds and enable comparison the antibacterial effect of the different formulations.

Hydrogels are viscous fluid, and as a result difficult to pipette in a precise manner. For the empty chitosan hydrogel, bacterial inhibition zones for *E.coli* showed signs of air bubbles inside applied sample (Appendix II). This may have caused a larger area of direct contact between bacteria covered agar plate and hydrogel formulation and could have resulted in an overestimation of the inhibition.

9 Conclusion

The aim of this project was to develop a drug delivery system with both antimicrobial and wound healing properties, intended for the treatment of skin infections and chronic wounds. To achieve this, both chlorogenic acid and a synthetic mimic of an antimicrobial peptide were incorporated into a liposome-in-hydrogel with the bioactive polymer chitosan.

Both the liposomal suspensions and the liposome-in-hydrogel system were tested over a 12-week period to assure applicability for dermal drug delivery and stability over time. The dual-loaded liposomes were found to have good stability and appropriate properties for dermal application. They also had a superior entrapment of active compounds compared to single-loaded liposomes. Hydrogel attributes, such as pH, viscosity and texture properties, were also considered appropriate for wound application. The liposome-in-hydrogel delivery system appear to be a suitable drug delivery system for the SMAMP 8b, exhibiting good stability, effective entrapment and a sustained release over 24 hours.

However, further testing is required to assure effect and safety of the dual-loaded formulation. The insufficient CGA release from the liposome-in-hydrogel formulation will be a limiting factor for desired therapeutic effect if not further explored or resolved. It is also important to assure that CGA and the hydrogel formulation does not induce toxicity in immune- or skin cells, disrupting the skin healing process. Finally, the antimicrobial activity should be explored with another method of determination than the modified disc-diffusion method.

Based on the findings of this thesis, the liposome-in-hydrogel formulation has potential as a dual drug delivery system for treatment of chronic wounds. The system shows good compatibility with the SMAMP 8b, but the effect and safety related to the release, stability and cell toxicity of CGA must be further investigated.

10 Perspectives

Short-term perspectives:

- Anti-inflammatory testing on macrophages by determining the drug formulation's ability of inhibiting LPS-induced production of pro-inflammatory mediators, such as NO, TNF- α and IL-6
- Further antibacterial evaluation to determine activity of CGA and 8b
- Toxicity studies on other relevant cell lines, such as keratinocytes and fibroblasts, in addition to further evaluation of the effect of CGA on cell viability.
- Morphological evaluations of liposomes through methods such as TEM
- Quantification of phospholipids to determine possible loss in extrusion process
- Cell migration studies by *in vitro* scratch assay
- *Ex vivo* studies on skin testing bioadhesion or drug permeation
- Testing of biofilm eradication and inhibition of biofilm development, both *in vitro* and *ex vivo*

Long-term perspectives:

- *In vivo* animal studies to assess the effects and safety of drug delivery formulation

11 References

1. Hemmingsen LM, Škalko-Basnet N, Jøraholmen MW. The Expanded Role of Chitosan in Localized Antimicrobial Therapy. *Mar Drugs* 2021;19(12):697.
2. Pfalzgraff A, Brandenburg K, Weindl G. Antimicrobial Peptides and Their Therapeutic Potential for Bacterial Skin Infections and Wounds. *Front Pharmacol* 2018;9:281.
3. Zhao R, Liang H, Clarke E, Jackson C, Xue M. Inflammation in Chronic Wounds. *Int J Mol Sci* 2016;17(12):2085.
4. Drago F, Gariazzo L, Cioni M, Trave I, Parodi A. The microbiome and its relevance in complex wounds. *Eur J Dermatol* 2019;29(1):6-13.
5. Velnar T, Bailey T, Smrkolj V. The Wound Healing Process: an Overview of the Cellular and Molecular Mechanisms. *J Int Med Res* 2009;37(5):1528-42.
6. Paulsen MH, Engqvist M, Ausbacher D, Anderssen T, Langer MK, Haug T, et al. Amphipathic Barbiturates as Mimics of Antimicrobial Peptides and the Marine Natural Products Eusynstyelamides with Activity against Multi-resistant Clinical Isolates. *J Med Chem* 2021;64(15):11395-417.
7. Akbarzadeh A, Rezaei-Sadabady R, Davaran S, Joo SW, Zarghami N, Hanifehpour Y, et al. Liposome: classification, preparation, and applications. *Nanoscale Res Lett* 2013;8(1):1-9.
8. Danaei M, Dehghankhold M, Ataei S, Davarani FH, Javanmard R, Dokhani A, et al. Impact of Particle Size and Polydispersity Index on the Clinical Applications of Lipidic Nanocarrier Systems. *Pharmaceutics* 2018;10(2):57.
9. Jøraholmen MW, Basnet P, Tostrup MJ, Moueffaq S, Skalko-Basnet N. Localized Therapy of Vaginal Infections and Inflammation: Liposomes-In-Hydrogel Delivery System for Polyphenols. *Pharmaceutics* 2019;11(2):53.
10. Hemmingsen LM, Julin K, Ahsan L, Basnet P, Johannessen M, Skalko-Basnet N. Chitosomes-In-Chitosan Hydrogel for Acute Skin Injuries: Prevention and Infection Control. *Mar Drugs* 2021;19(5):269.
11. Hurler J, Engesland A, Poorahmary Kermany B, Škalko-Basnet N. Improved texture analysis for hydrogel characterization: Gel cohesiveness, adhesiveness, and hardness. *J Appl Polym Sci* 2012;125(1):180-8.
12. Smith R, Russo J, Fiegel J, Brogden N. Antibiotic Delivery Strategies to Treat Skin Infections When Innate Antimicrobial Defense Fails. *Antibiotics* 2020;9(2):56.
13. Khan F, Pham DTN, Oloketuyi SF, Manivasagan P, Oh J, Kim Y-M. Chitosan and their derivatives: Antibiofilm drugs against pathogenic bacteria. *Colloids Surf B* 2020;185:110627.
14. Dash M, Chiellini F, Ottenbrite RM, Chiellini E. Chitosan—A versatile semi-synthetic polymer in biomedical applications. *Prog Polym Sci* 2011;36(8):981-1014.
15. El Maghraby GM, Barry BW, Williams AC. Liposomes and skin: From drug delivery to model membranes. *Eur J Pharm Sci* 2008;34(4):203-22.
16. Lai F, Caddeo C, Manca ML, Manconi M, Sinico C, Fadda AM. What's new in the field of phospholipid vesicular nanocarriers for skin drug delivery. *Int J Pharm* 2020;583:119398.
17. Lee SH, Jeong SK, Ahn SK. An Update of the Defensive Barrier Function of Skin. *Yonsei Med J* 2006;47(3):293-306.
18. Tomic-Canic M, Burgess JL, O'Neill KE, Strbo N, Pastar I. Skin Microbiota and its Interplay with Wound Healing. *Am J Clin Dermatol* 2020;21(1):36-43.

19. Tottoli EM, Dorati R, Genta I, Chiesa E, Pisani S, Conti B. Skin Wound Healing Process and New Emerging Technologies for Skin Wound Care and Regeneration. *Pharmaceutics* 2020;12(8):735.
20. Than UTT, Guanzon D, Leavesley D, Parker T. Association of Extracellular Membrane Vesicles with Cutaneous Wound Healing. *Int J Mol Sci* 2017;18(5):956.
21. Tognetti L, Martinelli C, Berti S, Hercogova J, Lotti T, Leoncini F, et al. Bacterial skin and soft tissue infections: review of the epidemiology, microbiology, aetiopathogenesis and treatment: a collaboration between dermatologists and infectivologists. *J Eur Acad Dermatol Venereol* 2012;26(8):931-41.
22. Rubey KM, Brenner JS. Nanomedicine to fight infectious disease. *Adv Drug Deliv Rev* 2021;179:113996.
23. Hemmingsen LM, Giordani B, Pettersen AK, Vitali B, Basnet P, Škalko-Basnet N. Liposomes-in-chitosan hydrogel boosts potential of chlorhexidine in biofilm eradication in vitro. *Carbohydr Polym* 2021;262:117939.
24. Hurler J, Sørensen KK, Fallarero A, Vuorela P, Škalko-Basnet N. Liposomes-in-Hydrogel Delivery System with Mupirocin: In Vitro Antibiofilm Studies and In Vivo Evaluation in Mice Burn Model. *Biomed Res Int* 2013;2013:498485.
25. Omar A, Wright JB, Schultz G, Burrell R, Nadworny P. Microbial Biofilms and Chronic Wounds. *Microorganisms* 2017;5(1):9.
26. Funari R, Shen AQ. Detection and Characterization of Bacterial Biofilms and Biofilm-Based Sensors. *ACS Sens* 2022;7(2):347-57.
27. Murugaiyan J, Kumar PA, Rao GS, Iskandar K, Hawser S, Hays JP, et al. Progress in Alternative Strategies to Combat Antimicrobial Resistance: Focus on Antibiotics. *Antibiotics (Basel)* 2022;11(2):200.
28. Sgolastra F, deRonde BM, Sarapas JM, Som A, Tew GN. Designing Mimics of Membrane Active Proteins. *Acc Chem Res* 2013;46(12):2977-87.
29. Bahar AA, Ren D. Antimicrobial peptides. *Pharmaceutics* 2013;6(12):1543-75.
30. Langenegger N, Nentwig W, Kuhn-Nentwig L. Spider Venom: Components, Modes of Action, and Novel Strategies in Transcriptomic and Proteomic Analyses. *Toxins* 2019;11(10):611.
31. Wang D-Y, van der Mei HC, Ren Y, Busscher HJ, Shi L. Lipid-Based Antimicrobial Delivery-Systems for the Treatment of Bacterial Infections. *Front Chem* 2020;7:872.
32. Moghadam SE, Ebrahimi SN, Salehi P, Farimani MM, Hamburger M, Jabbarzadeh E. Wound Healing Potential of Chlorogenic Acid and Myricetin-3-O-beta-Rhamnoside Isolated from *Parrotia persica*. *Molecules* 2017;22(9):1501.
33. Navarro-Orcajada S, Matencio A, Vicente-Herrero C, Garcia-Carmona F, Manuel Lopez-Nicolas J. Study of the fluorescence and interaction between cyclodextrins and neochlorogenic acid, in comparison with chlorogenic acid. *Sci Rep* 2021;11(1):3275.
34. Li G, Wang X, Xu Y, Zhang B, Xia X. Antimicrobial effect and mode of action of chlorogenic acid on *Staphylococcus aureus*. *Eur Food Res Technol* 2014;238(4):589-96.
35. Lou Z, Wang H, Zhu S, Ma C, Wang Z. Antibacterial Activity and Mechanism of Action of Chlorogenic Acid. *J Food Sci* 2011;76(6):M398-M403.
36. Nwafor E-O, Lu P, Zhang Y, Liu R, Peng H, Xing B, et al. Chlorogenic acid: Potential source of natural drugs for the therapeutics of fibrosis and cancer. *Transl Oncol* 2022;15(1):101294.
37. Hua S. Lipid-based nano-delivery systems for skin delivery of drugs and bioactives. *Front Pharmacol* 2015;6:219.
38. du Plessis J, Ramachandran C, Weiner N, Müller DG. The influence of particle size of liposomes on the deposition of drug into skin. *Int J Pharm* 1994;103(3):277-82.

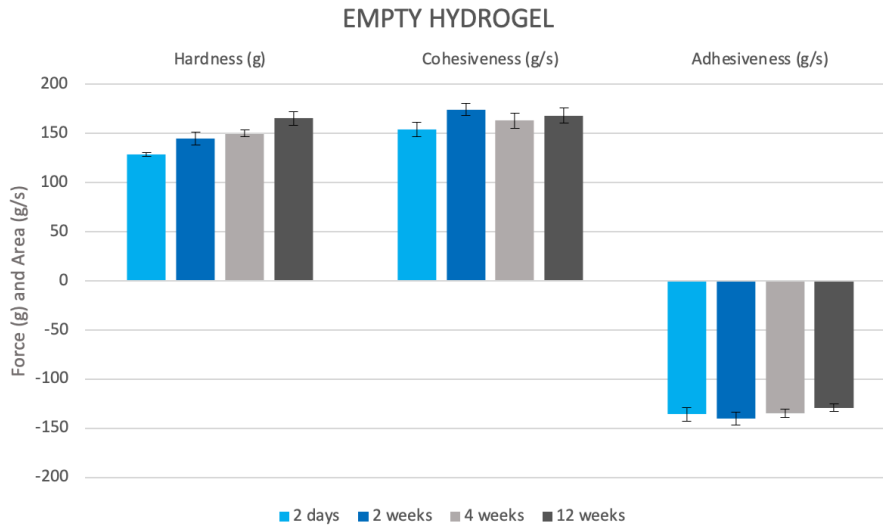
39. Ahmed KS, Hussein SA, Ali AH, Korma SA, Lipeng Q, Jinghua C. Liposome: composition, characterisation, preparation, and recent innovation in clinical applications. *J Drug Target* 2019;27(7):742-61.
40. Guimarães D, Cavaco-Paulo A, Nogueira E. Design of liposomes as drug delivery system for therapeutic applications. *Int J Pharm* 2021;601:120571.
41. Hurler J, Berg OA, Skar M, Conradi AH, Johnsen PJ, Škalko - Basnet N. Improved Burns Therapy: Liposomes - in - Hydrogel Delivery System for Mupirocin. *J Pharm Sci* 2012;101(10):3906-15.
42. Contini C, Schneemilch M, Gaisford S, Quirke N. Nanoparticle-membrane interactions. *J Exp Nanosci* 2018;13(1):62-81.
43. Soares S, Sousa J, Pais A, Vitorino C. Nanomedicine: Principles, Properties, and Regulatory Issues. *Front Chem* 2018;6:360.
44. Indiarito R, Indriana LPA, Andoyo R, Subroto E, Nurhadi B. Bottom-up nanoparticle synthesis: a review of techniques, polyphenol-based core materials, and their properties. *Eur Food Res Technol* 2021;248(1):1-24.
45. Modena MM, Rühle B, Burg TP, Wuttke S. Nanoparticle Characterization: Nanoparticle Characterization: What to Measure? . *Adv Mater* 2019;31(32):1970226.
46. Balzus B, Colombo M, Sahle FF, Zoubari G, Staufenbiel S, Bodmeier R. Comparison of different in vitro release methods used to investigate nanocarriers intended for dermal application. *Int J Pharm* 2016;513(1-2):247-54.
47. Liu H, Wang C, Li C, Qin Y, Wang Z, Yang F, et al. A functional chitosan-based hydrogel as a wound dressing and drug delivery system in the treatment of wound healing. *RSC Adv* 2018;8(14):7533-49.
48. Hurler J, Skalko-Basnet N. Potentials of chitosan-based delivery systems in wound therapy: bioadhesion study. *J Funct Biomater* 2012;3(1):37-48.
49. Hupfeld SH, Ann Mari; Skar, Merete; Frantzen, Christer B.; Brandl, Martin Liposome size analysis by dynamic/static light scattering upon size exclusion-/field flow-fractionation. *J Nanosci Nanotechnol* 2006;6.
50. Pedersen AK. Liposomal formulations for membrane active antimicrobials - Assuring safety through an optimised drug delivery system: UiT - The Arctic University of Norway; 2020.
51. Balouiri M, Sadiki M, Ibsouda SK. Methods for in vitro evaluating antimicrobial activity: A review. *J Pharm Anal* 2016;6(2):71-9.
52. Jøraholmen MW, Bhargava A, Julin K, Johannessen M, Skalko-Basnet N. The Antimicrobial Properties of Chitosan Can Be Tailored by Formulation. *Mar Drugs* 2020;18(2):96.
53. Schulte-Werning LV, Murugaiah A, Singh B, Johannessen M, Engstad RE, Skalko-Basnet N, et al. Multifunctional Nanofibrous Dressing with Antimicrobial and Anti-Inflammatory Properties Prepared by Needle-Free Electrospinning. *Pharmaceutics* 2021;13(9):1527.
54. Schneider CA, Rasband WS, Eliceiri KW. NIH Image to ImageJ: 25 years of image analysis. *Nat Methods* 2012;9(7):671-5.
55. Carvalho FC, Calixto G, Hatakeyama IN, Luz GM, Gremião MPD, Chorilli M. Rheological, mechanical, and bioadhesive behavior of hydrogels to optimize skin delivery systems. *Drug Dev Ind Pharm* 2013;39(11):1750-7.
56. Saghadzadeh S, Rinoldi C, Schot M, Kashaf SS, Sharifi F, Jalilian E, et al. Drug delivery systems and materials for wound healing applications. *Adv Drug Deliv Rev* 2018;127:138-66.
57. Standardization IOF. Biological evaluation of medical devices. Part 5: Tests for in vitro cytotoxicity: ISO; 2009.

58. Tincer GB, Banu; Arica, Yakup M.; Gürsel, Ihsan. Chitosan Polysaccharide Suppress Toll Like Receptor Dependent Immune Response. Turk J Immunol 2015;3(1):15-20.

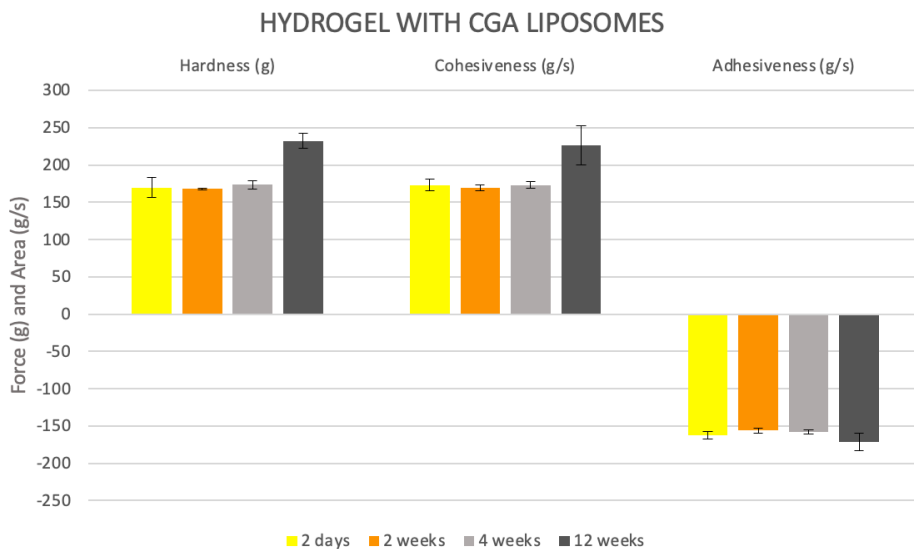
12 Appendix

Appendix I: Stability testing of texture properties

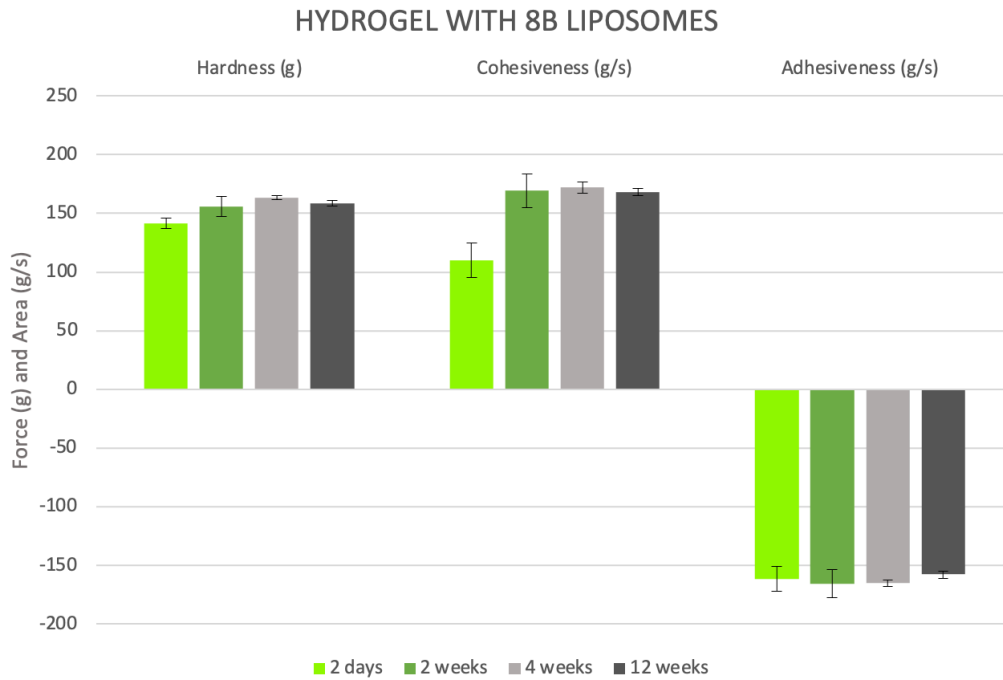
Appendix Figure 1-4 shows the texture properties of the chitosan hydrogel, both empty and loaded, over the stability testing period of 12 weeks.



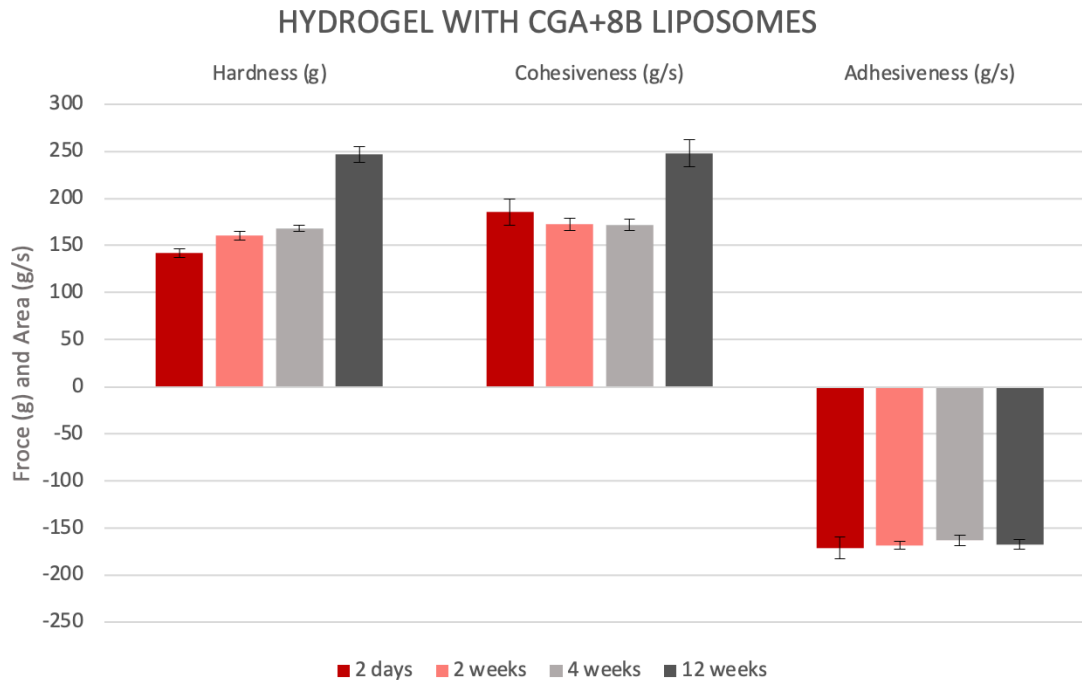
Appendix Figure 1: Texture properties of empty chitosan hydrogel over a period of 12 weeks after production. Results are presented as mean \pm SD, n=3.



Appendix Figure 2: Texture properties of chitosan hydrogel with incorporated CGA-liposomes over a period of 12 weeks after production. Results are presented as mean \pm SD, n=3.



Appendix Figure 3: Texture properties of chitosan hydrogel with incorporated 8b-liposomes over a period of 12 weeks after production. Results are presented as mean \pm SD, n=3.

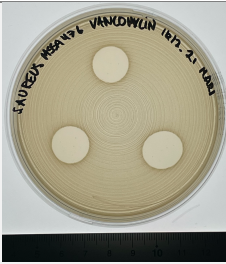
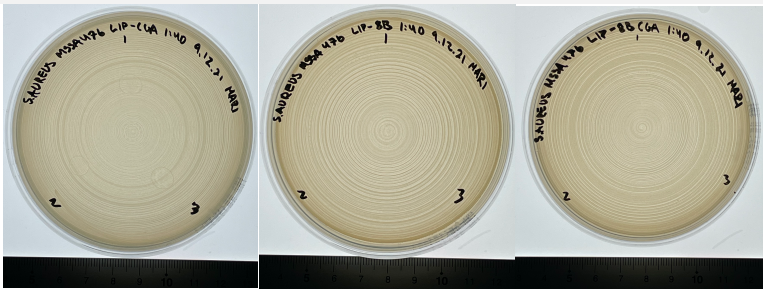
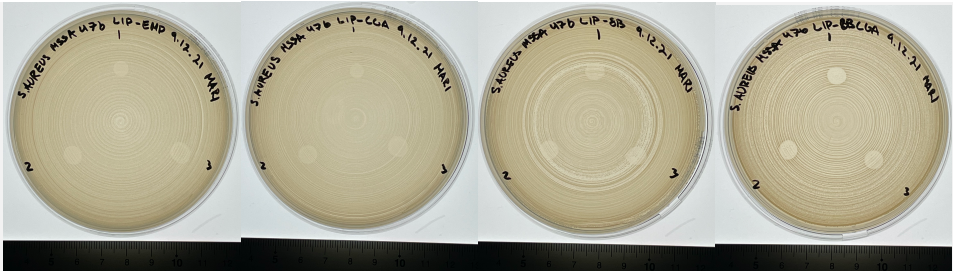
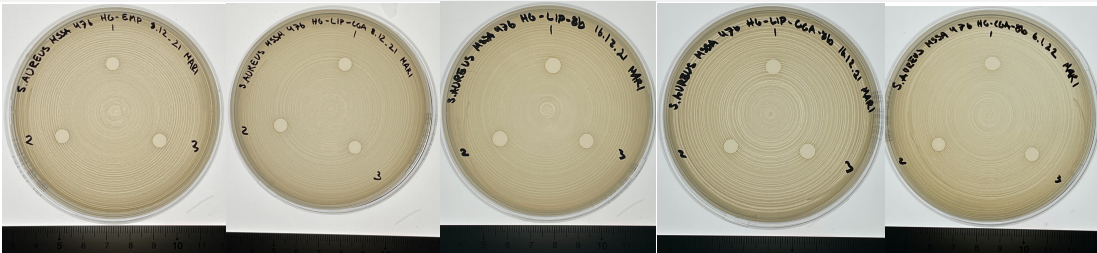


Appendix Figure 4: Texture properties of chitosan hydrogel with incorporated dual-loaded 8b-CGA-liposomes over a period of 12 weeks after production. Results are presented as mean \pm SD, n=3.

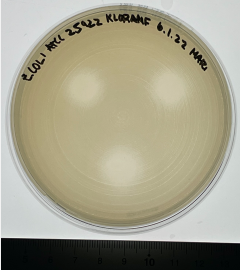
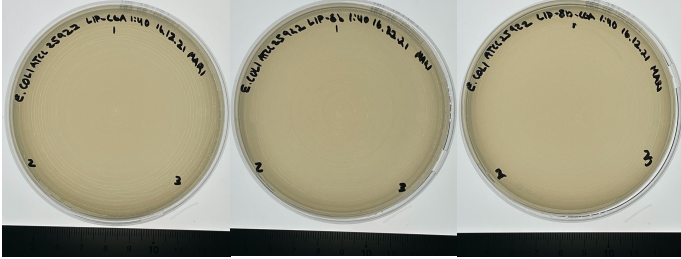
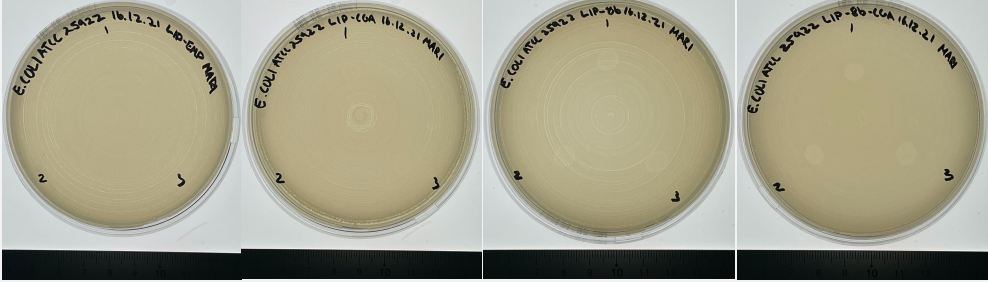
Appendix II: Antimicrobial testing

Appendix Table 1 and 2 shows the results from *in vitro* evaluation of antimicrobial activity on both *S. aureus* and *E. coli*. Evaluation was performed through the modified disc diffusion method as described in 7.12. Following pictures were taken after the 24 hours of incubation with applied formulations.

Appendix Table 1: Results from testing of antibacterial activity of liposomal suspensions and hydrogel formulations on *S. aureus*.

FORMULATION	RESULTS
CONTROL	
LIPOSOMES 1:40	
LIPOSOMES	
HYDROGEL 1:4	

Appendix Table 2: Results from testing of antibacterial activity of liposomal suspensions and hydrogel formulations on *E. coli*.

FORMULATION	RESULTS
CONTROL	
LIPOSOMES 1:40	
LIPOSOMES	
HYDROGEL 1:4	